Biochemical and Biophysical Research Communications 391 (2010) 1681–1686

Contents lists available at ScienceDirect

Biochemical and Biophysical Research Communications

journal homepage: www.elsevier.com/locate/ybbrc

Amino acid conditions near the GPI anchor attachment site of prion protein for the conversion and the GPI anchoring

Masaki Hizume [a,b], Atsushi Kobayashi [a], Hidehiro Mizusawa [b], Tetsuyuki Kitamoto [a,*]

[a] Division of CJD Science and Technology, Department of Prion Research, Tohoku University Graduate School of Medicine, 2-1 Seiryo-machi, Aoba-ku, Sendai 980-8575, Japan
[b] Department of Neurology and Neurological Science, Graduate School, Tokyo Medical and Dental University, Tokyo 113-8519, Japan

ARTICLE INFO

Article history:
Received 15 December 2009
Available online 29 December 2009

Keywords:
Prion protein
Mutation
Glycosylphosphatidylinositol anchor
Conversion
ω Site

ABSTRACT

Prion protein (PrP) is a glycosylphosphatidylinositol (GPI)-anchored protein, and the C-terminal GPI anchor signal sequence (GPI-SS) of PrP is cleaved before GPI anchoring. However, mutations near the GPI anchor attachment site (the ω site) in the GPI-SS have been recognized in human genetic prion diseases. Moreover, the ω site of PrP has not been identified except hamster, though it is known that amino acid restrictions are very severe at the ω and ω + 2 sites in other GPI-anchored proteins. To investigate the effect of mutations near the ω site of PrP on the conversion and the GPI anchoring, and to discover the ω site of murine PrP, we systematically created mutant murine PrP with all possible single amino acid substitutions at every amino acid residue from codon 228 to 240. We transfected them into scrapie-infected mouse neuroblastoma cells and examined the conversion efficiencies and the GPI anchoring of each mutant PrP. Mutations near the ω site altered the conversion efficiencies and the GPI anchoring efficiencies. Especially, amino acid restrictions for the conversion and the GPI anchoring were severe at codons 230 and 232 in murine PrP, though they were less severe than in other GPI-anchored proteins. Only the mutant PrPs presented on a cell surface via a GPI anchor were conversion competent. The present study shows that mutations in the GPI-SS can affect the GPI anchoring and the conversion efficiency of PrP. We clarified for the first time the ω site of murine PrP and the amino acid conditions near the ω site for the conversion as well as GPI anchoring.

Introduction

Prion diseases are infectious fatal neurodegenerative diseases that include scrapie in sheep and goat, bovine spongiform encephalopathy in cattle and Creutzfeldt–Jakob disease (CJD) in human, which are caused by infectious abnormal prion protein (PrP^{Sc}) that is converted from the normal cellular prion protein (PrP^{C}) [1].

PrP^{C} is attached to a cell surface via a glycosylphosphatidylinositol (GPI) anchor [2]. Shortly after the precursor PrP is fully translocated into the ER lumen, a GPI anchor is added rapidly to the acceptor amino acid, termed the ω site [3], following the cleavage of the C-terminal GPI anchor signal sequence (GPI-SS) by the action of a GPI transamidase [4].

More than 30 causative mutations in human genetic prion diseases have been recognized so far [5]. Among them, the amino acid substitutions of M232R [6–8] and M232T [9] have been reported as mutations in the GPI-SS. However, the GPI-SS is not included in the mature PrP as a consequence of a posttranslational modification, which raises a question about the effect of the mutation in the GPI-SS on the conversion of PrP.

Meanwhile, a database analysis revealed that the GPI-SS of GPI-anchored proteins has several general features but does not contain any consensus sequence [10]. In addition, the ω site of PrP has been identified only in hamster [11], of which the amino acid residues near the ω site are somewhat different from those of mouse. Therefore, the ω site of murine PrP has been only assumed to be codon 230 [4] or 231 [12] but not determined accurately, and the amino acid conditions of the GPI-SS for GPI anchoring need to be examined thoroughly.

In the present study, to investigate the effects of a single amino acid substitution near the ω site of PrP on the conversion and the GPI anchoring, we systematically examined the conversion efficiency and the GPI anchor attachment of mutant murine PrP with all possible single amino acid substitutions at every amino acid residue from codon 228 to 240 in scrapie-infected mouse neuroblastoma (ScN2a) cells. We revealed the amino acid conditions in the GPI-SS of PrP necessary for the conversion and the GPI anchor attachment and identified the ω site of murine PrP.

Materials and methods

Cell culture. ScN2a cells were kindly provided by Dr. Stanley B. Prusiner [13] and maintained in Dulbecco's modified Eagle's med-

* Corresponding author. Fax: +81 22 717 8148.
E-mail address: kitamoto@mail.tains.tohoku.ac.jp (T. Kitamoto).

0006-291X/$ - see front matter © 2009 Elsevier Inc. All rights reserved.
doi:10.1016/j.bbrc.2009.12.128

ium (Invitrogen) containing 10% fetal bovine serum (Invitrogen), 100 U/ml penicillin and 100 μg/ml streptomycin (Invitrogen) at 37 °C in 5% CO_2.

Plasmid construction. The open reading frame of mouse PrP gene was cloned into plasmid pBluescript (Stratagene) as described [14]. The epitope for the monoclonal antibody 3F4 (L108M and V111M) [15] and 19 kinds of single amino acid substitutions at every amino acid residue from codon 228 to 240 were introduced into mouse PrP gene by site-directed PCR mutagenesis as described [14]. These 3F4 epitope-tagged mutant PrP fragments were cloned into the expression vector pSPOX [16]. All amino acid numbers refer to mouse PrP sequence.

Transfection and harvest. ScN2a cells were transiently transfected with plasmid constructs using the FuGENE® 6 transfection reagent according to the manufacturer's directions (Roche Diagnostics). The medium was exchanged after 24 h of transfection. After 48 h of transfection, the cells were harvested with 1 ml of lysis buffer (10 mM Tris–HCl pH 7.5, 100 mM NaCl, 1 mM EDTA, 0.5% Triton X-100, and 0.5% sodium deoxycholate) and the cell debris and nuclei were removed by low-speed centrifugation.

Deglycosylation treatment. For the detection of the total cell-associated PrP (PrP^{total}), 20 μl of the cell lysates were boiled with the addition of 5 μl of 5 × sample buffer (10% SDS, 300 mM Tris–HCl pH 6.8, 25% 2-mercaptoethanol, 25% glycerol, and 0.05% bromophenol blue), and digested with 300 U of PNGase F (New England Biolabs) at 37 °C for 2 h. For the evaluation of the sensitivity to Endoglycosidase H treatment, 20 μl of the cell lysates were boiled with the addition of 5 μl of 5 × sample buffer and digested with 500 U of Endoglycosidase H (New England Biolabs) at 37 °C for 2 h.

Protease treatment. For the detection of the proteinase K (PK) resistant form of PrP (PrP^{res}), 480 μl of the cell lysates were digested with 20 μg/ml PK at 37 °C for 30 min in the presence of 2% sarkosyl. The digestion was terminated by adding 2 mM of Pefabloc SC (Roche Diagnostics). The digested samples were ultracentrifuged at 100,000g, 20 °C for 1 h, and the pellets were resuspended with 40 μl of sample buffer and boiled.

Phosphatidylinositol-phospholipase C (PI-PLC) treatment. Subconfluent ScN2a cells in 6-well plates were transiently transfected with plasmid constructs as described above. The medium was exchanged after 24 h of transfection. After 45 h of transfection, the medium was removed, and 1 ml of PBS containing 0.25 U of PI-PLC (Sigma–Aldrich Inc.) was added for the detection of the PrP released from the cell membrane. The cells were incubated with PI-PLC at 37 °C for 3 h before the culture supernatants were harvested. For a negative control, the cells were incubated with 1 ml of PBS. Detached cells, if any, were removed by low-speed centrifugation. For the detection of the released PrP, 40 μl of the supernatants were digested with PNGase F for the deglycosylation as described above.

Triton X-114 phase-partitioning. ScN2a cells in 10-cm dishes were washed with PBS and harvested with 1 ml of Triton X-114 lysis buffer (10 mM Tris–HCl pH 7.5, 100 mM NaCl, 1 mM EDTA, and 2% Triton X-114). These cell lysates were incubated at 4 °C for 10 min and centrifuged at 1500g, 4 °C for 5 min to pellet cell debris and nuclei. For the Triton X-114 phase-partitioning, 400 μl of the supernatants were incubated at 37 °C for 10 min and centrifuged at 9000g, 37 °C for 10 min. The upper aqueous phases were mixed with equal volume (360 μl) of Triton X-114 lysis buffer, and boiled with the addition of 180 μl of 5 × sample buffer. The lower Triton X-114 phases were mixed with 360 μl of TNE buffer (10 mM Tris–HCl pH 7.5, 100 mM NaCl, 1 mM EDTA) and incubated at 4 °C for 5 min. The phase-partitioning step was repeated two times to wash the detergent phases thoroughly. The Triton X-114 phases were mixed with 680 μl of TNE buffer, and boiled with the addition of 180 μl of 5 × sample buffer. The boiled samples were digested with PNGase F for the deglycosylation as described above.

Western blot analysis. The samples were applied to 13% SDS–PAGE and Western blotting using monoclonal antibody 3F4 (Signet Laboratories) as described [14,17]. To calculate the relative conversion efficiency of mutant PrP, the relative expression level of PrP^{res} was divided by that of PrP^{total}. All experiments were repeated independently at least three times, and representative data are shown.

Results

Single amino acid substitutions near the ω site of PrP alter the conversion efficiency, and the amino acid restrictions for the conversion are very severe at codons 230 and 232.

We first addressed the question of whether single amino acid substitutions near the ω site of PrP gene might alter the conversion efficiency. We created mutant murine PrP constructs with all possible single amino acid substitutions at every amino acid residue from codon 228 to 240 and transfected them into ScN2a cells. By the Western blot analysis, we observed the following: (i) at codons 228 and 229, each expression level of the mutant PrP^{total} was almost equal to that of WT PrP^{total} (Fig. 1A and C, gray bars; Supplementary Fig. 1A and C, gray bars), whereas the conversion efficiencies of mutant PrP substituted with C, D, E, F, W or Y at codon 228, or with D, E, F or W at codon 229 were decreased to 0.2 or less compared to that of WT PrP (Fig. 1B and D, black bars; Supplementary Fig. 1B and D, black bars); (ii) at codon 230, the relative conversion efficiencies of each PrP substituted with C, E, F, H, I, K, L, M, Q, R, W or Y were reduced to 0.2 or less (Fig. 1H and J, black bars), of which the expression levels of PrP^{total} were also relatively decreased (Fig. 1G and I, gray bars). In contrast, the relative conversion efficiencies of each PrP substituted with A, D, G, N, P, T or V were generally sustained (Fig. 1H and J, white bars), and the expression levels of PrP^{total} were also relatively maintained (Fig. 1G and I, gray bars); (iii) at codon 231, the relative expression levels of the mutant PrP^{total} only modestly varied (Fig. 1K and M, gray bars), while the relative conversion efficiency of the mutant PrP was decreased to 0.2 or less only in S231W (Fig. 1L and N, black bar); (iv) at codon 232, the relative conversion efficiencies of each PrP substituted with F, I, L, M, P, W or Y were reduced to 0.2 or less (Fig. 1R and T, black bars), and the expression levels of PrP^{total} were also relatively decreased (Fig. 1Q and S, gray bars). In contrast, the relative conversion efficiencies of each PrP substituted with A, C, D, E, G, H, K, N, Q, R, T or V were generally sustained (Fig. 1R and T, white bars), and the expression levels of PrP^{total} were also relatively maintained (Fig. 1Q and S, gray bars); (v) at every residue from codon 233 to 240, single amino acid substitutions hardly affected the conversion efficiencies of the mutant PrP or the expression levels of the mutant PrP^{total} (Supplementary Fig. 1E–j). Taken

Fig. 1. Single amino acid substitutions near the ω site of PrP can alter the conversion efficiency, and the amino acid restrictions for the conversion are very severe at codons 230 and 232 in murine PrP. (A, G, K, Q) Western blot analysis for the PrP^{total} of WT and mutations at codon 228, 230, 231 or 232, respectively, after deglycosylation with PNGase F. (B, H, L, R) Western blot analysis for the PrP^{res} of WT and mutations at codon 228, 230, 231 or 232, respectively. (C, I, M, S) The relative expression levels of mutant PrP^{total} (gray bars) and those of mutant PrP^{res} (black bars) at codon 228, 230, 231 or 232, respectively. (D, J, N, T) The relative conversion efficiencies at codon 228, 230, 231 or 232, respectively. Black bars indicate the relative conversion efficiencies reduced to 0.2 or less. (E, O) Western blot analysis for the PrP^{total} of WT and mutations at codon 230 or 232, respectively, without deglycosylation. (F, P) Western blot analysis for the PrP^{total} of WT and mutations at codon 230 or 232, respectively, after deglycosylation with Endoglycosidase H. In A, B, E–H, K, L, and O–R, molecular size markers are indicated as bars on the left side of the panels and represent 32.5, 25 and 16.5 kDa. In C, D, I, J, M, N, S and T, data represent mean ± standard deviation of three independent experiments.

together, the single amino acid substitutions near the ω site in the GPI-SS of murine PrP altered the relative expression levels as well as the relative conversion efficiencies. The amino acid restrictions for the conversion were very severe at codons 230 and 232.

The amino acid substitutions at codon 230 or 232 of PrP markedly affected the expression levels of PrP^{total} and the conversion efficiencies. Therefore, we next examined the sensitivity of N-linked glycans on each mutant PrP to Endoglycosidase H treat-

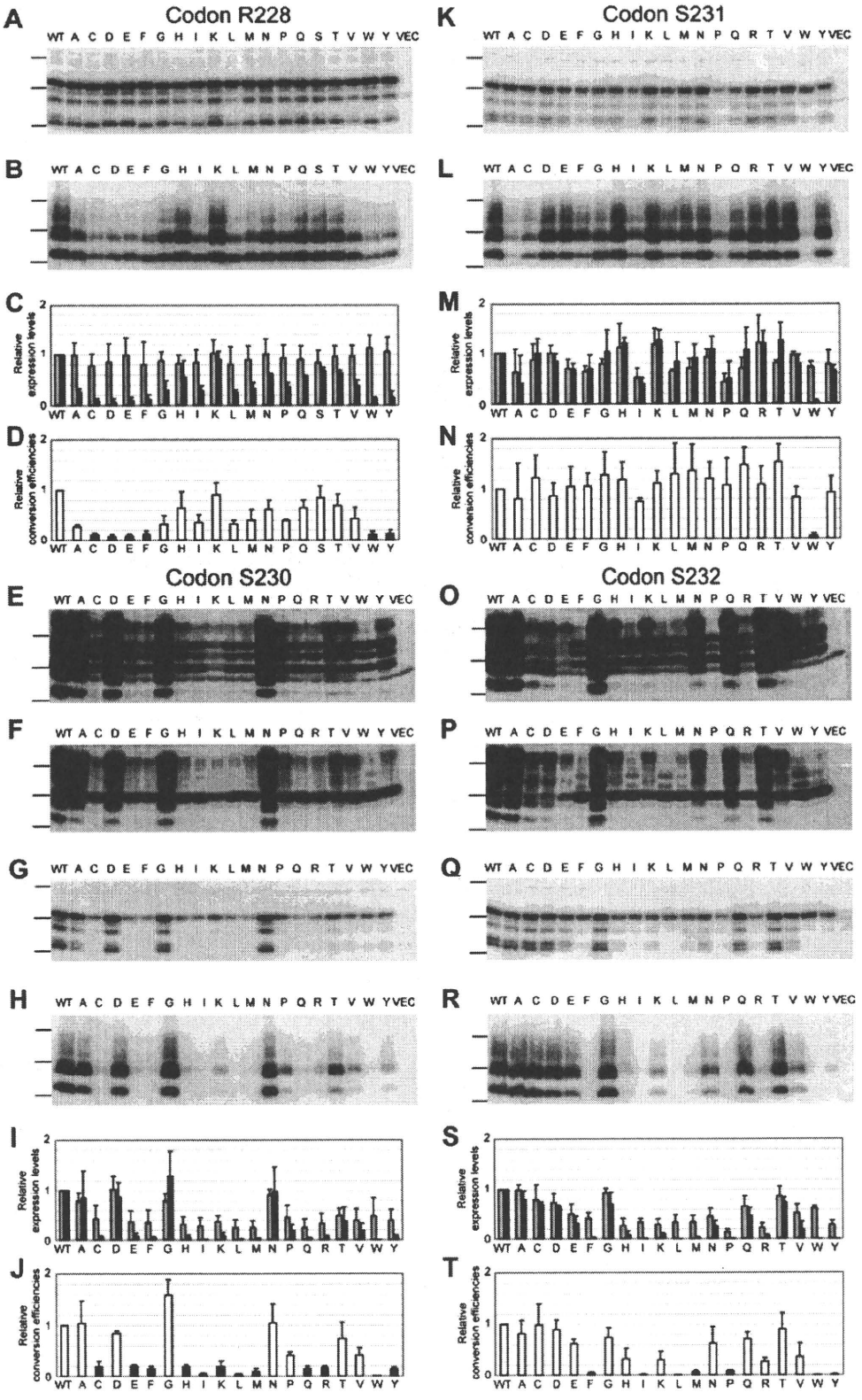

ment. If mutant PrP is misfolded and retained in the ER, the N-linked glycans on the mutant PrP should be the high mannose-type and cleaved by Endoglycosidase H. At codon 230, only the N-linked glycans of mutant PrP substituted with A, D, G, N or T were resistant to Endoglycosidase H treatment (Fig. 1E and F). At codon 232, the N-linked glycans of mutant PrP substituted with A, C, D, G, N, Q, T or V were resistant to Endoglycosidase H (Fig. 1O and P). These results suggest that the amino acid substitutions at codon 230 or 232 can cause the retention of mutant PrP in the ER and result in decreased expression levels of PrP^{total}.

Only GPI-anchored mutant PrP can be converted into PrP^{res}

The severe restrictions for the conversion at codons 230 and 232 raised the possibility that codon 230 was the ω site and codon 232 was the ω + 2 site in murine PrP. To address this possibility, we next analyzed the GPI anchoring of the mutant PrP by PI-PLC treatment. If mutant PrP is attached to a cell membrane via a GPI anchor, PI-PLC treatment of the cells results in release of the membrane-anchored PrP into the medium. The Western blot analysis of the incubation medium revealed the following: (i) at codon 228, PI-PLC cleaved all the mutant PrP as well as WT PrP (Fig. 2A); (ii) at codon 230, PI-PLC cleaved the mutant PrP substituted with A, D, G, N, P, T or V (Fig. 2B); (iii) at codon 232, PI-PLC cleaved the mutant PrP substituted with A, C, D, E, G, H, K, N, Q, R, T or V (Fig. 2C).

Since the N-linked glycans of most mutant PrPs with amino acid substitutions at codon 230 or 232 were sensitive to Endoglycosidase H treatment (Fig. 1F and P), there remained the possibility that the mutant PrPs were just misfolded and retained in the ER and could not be released by PI-PLC even if they were GPI-anchored. To address this possibility, we next performed Triton X-114 phase-partitioning to isolate GPI-anchored PrP. If mutant PrPs

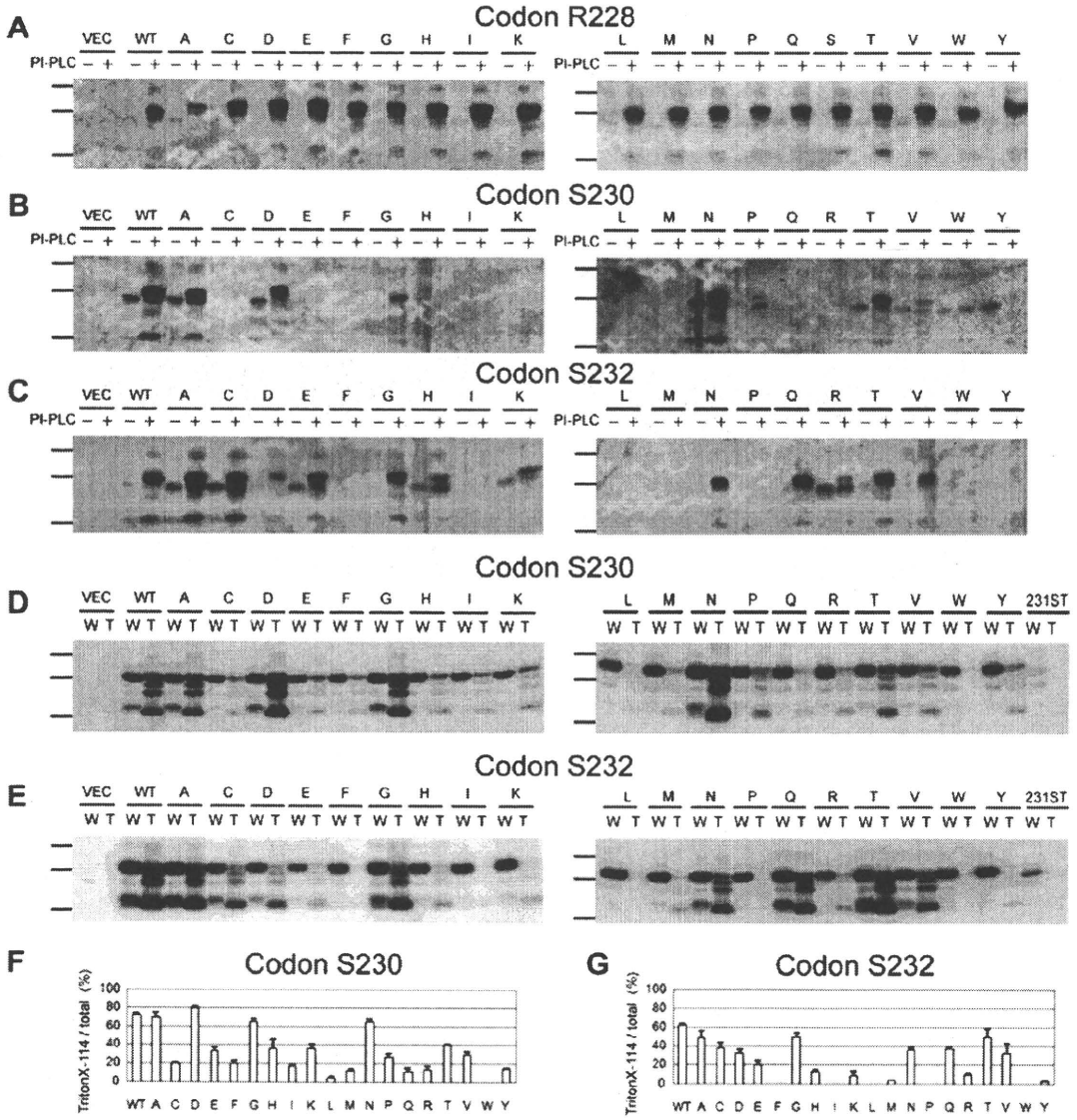

Fig. 2. Single amino acid substitutions near the ω site of PrP can alter the GPI anchoring efficiency, and the amino acid conditions for the anchoring are very tight at codons 230 and 232 in murine PrP. (A–C) The bands of released PrP were detected in WT and some mutations at codon 228, 230 or 232, respectively. Results are representative of several experiments repeated independently. (D, E) Triton X-114 phase-partitioning to isolate GPI-anchored PrP. W: water phase. T: Triton X-114 phase. 231ST: GPI-anchorless PrP with a stop codon after codon 231. (F, G) The proportion of GPI-anchored PrP in Triton X-114 phase-partitioning. Data represent mean ± standard deviation of three independent experiments. In A–E, molecular size markers are indicated as bars on the left side of the panels and represent 32.5, 25 and 16.5 kDa.

Table 1
Results are those of the comparison studies on the PrP conversion efficiencies/the released PrP with PI-PLC, respectively.

Substituting amino acids	Substituted position number of codons		
	228	230	232
W	−/+	−/−	−/−
Y	−/+	−/−	−/−
R	WT	−/−	+/+
F	−/+	−/−	−/−
H	+/+	−/−	+/+
M	+/+	−/−	−/−
E	−/+	−/−	+/+
K	+/+	−/−	+/+
Q	+/+	−/−	+/+
D	−/+	+/+	+/+
N	+/+	+/+	+/+
I	+/+	−/−	−/−
L	+/+	−/−	−/−
C	−/+	−/−	+/+
T	+/+	+/+	+/+
V	+/+	+/+	+/+
P	+/+	+/+	−/−
S	+/+	WT	WT
A	+/+	+/+	+/+
G	+/+	+/+	+/+

− means that the relative conversion efficiency of the mutant PrP was decreased to 0.2 or less, or that the mutant PrP was not released into the culture medium after PI-PLC treatment, respectively. + means that the relative conversion efficiency of the mutant PrP was sustained above 0.2 or that the mutant PrP was released into the culture medium after PI-PLC treatment, respectively.

are GPI-anchored, they should be collected within the Triton X-114 phase. At codon 230, only the mutant PrP substituted with A, D, G or N showed a relatively sustained Triton X-114/total PrP ratio compared to that of WT PrP (Fig. 2D and F). At codon 232, only the mutant PrP substituted with A, C, G, N, Q, T or V showed a relatively sustained Triton X-114/total PrP ratio (Fig. 2E and G). Therefore, we confirmed that the amino acid substitutions at codon 230 or 232 of murine PrP affected the GPI anchoring efficiencies.

Taken together, the single amino acid substitutions near the ω site of PrP altered the GPI anchoring efficiencies, and the amino acid conditions for the GPI anchoring were very tight at codons 230 and 232 in murine PrP. Furthermore, only the GPI-anchored mutant PrPs acquired resistance to the deglycosylation with Endoglycosidase H and could be converted into PrP^{res} (Table 1).

Discussion

Our study revealed three findings. First, the mutations near the ω site of PrP can alter not only the GPI anchoring efficiency but also the conversion efficiency. Second, amino acid conditions in the GPI-SS of murine PrP are very severe at codons 230 and 232 for the conversion as well as for the GPI anchoring. Finally, among mutant PrPs with amino acid substitutions in the GPI-SS, only the mutant PrPs presented on a cell surface via a GPI anchor are conversion competent. These results suggest that the loss of GPI anchoring might cause misfolding and ER-retention of the mutant PrP and result in the decreased expression level and the altered conversion efficiency.

The finding that amino acid restrictions for the GPI anchoring were very severe at codons 230 and 232 indicates that codons 230 and 232 are the ω and ω + 2 sites, respectively. A database analysis documented that the GPI-SS does not contain any consensus sequence but has several general features as follows [10]: (i) a stretch of ~10 polar amino acids (ω − 10 to ω − 1) that form a flexible linker region; (ii) amino acids of the ω site are those with small side-chains, such as G, A, S, N, D and C; (iii) the ω + 2 amino acids, the most restrictive position, are also those with small side-chains, such as G, A and S; (iv) a hydrophilic spacer region of moderately polar amino acids (ω + 3 to ω + 9 or more); and (v) a C-terminal hydrophobic sequence is variable in length but capable of spanning the membrane [3,18]. However, mutational studies with all possible single amino acid substitutions in the GPI-SS of GPI-anchored proteins have not been performed to date. Therefore, the amino acid conditions in the GPI-SS of PrP, especially near the ω site, for the GPI anchoring as well as for the conversion have not been examined completely. Our study revealed novel findings in the GPI-SS of PrP as follows: (i) at the ω site (codon 230), the amino acids essential for the GPI anchoring are not only G, A, S, N and D but also P, T and V (D or smaller amino acids except I, L and C); (ii) at the ω + 2 site (codon 232), they are C, D, E, H, K, N, Q, R, T and V as well as G, A and S (R or smaller amino acids excluding I, L, M, P and F). Taken together, these results suggest that the amino acid conditions at the ω and ω + 2 sites for the GPI anchoring are less severe in PrP than in other GPI-anchored proteins, though the amino acids at the ω site of PrP are more limited than those at the ω + 2 site (Table 1).

Amino acid substitutions in GPI-SS can alter GPI anchor attachment, and the mutant protein can be secreted into the culture medium [19] or retained in the ER [20]. Mutant PrP without the GPI anchor are secreted into the medium [21–23], while uncleaved GPI-SS causes retention of the PrP in the ER [24]. In addition, misfolded ER proteins can be degraded via a pathway termed ER-associated protein degradation [25], and a co-translocational or preemptive quality control pathway exists to reduce the burden of misfolded substrates entering the ER [26]. Since the mutant PrPs lacking GPI anchor were retained in the ER in this study, these mutant PrPs might be misfolded and degraded inside the ScN2a cells. Therefore, mutant PrPs lacking GPI anchor showed the decreased expression levels and the altered conversion efficiencies in the present study. Our finding that only the mutant PrPs presented on a cell surface via a GPI anchor are conversion competent indicates that PrP is converted after reaching the cell surface in ScN2a cells. Meanwhile, some mutant PrPs substituted at codon 228 or 229 showed decreased relative conversion efficiencies though they were GPI-anchored. At codons 228 and 229, substitutions with amino acids with negative or large side-chains might prevent the conversion of PrP independently of GPI anchoring as mutations in the core region of PrP reduced the conversion efficiency [14].

About 30 cases of genetic CJD with M232R have been reported so far [6–8], which accounts for about 13% of the genetic CJD patients in Japan. Therefore, the mutation is considered to be a causative mutation. Although the codon in murine PrP corresponding to codon 232 in human PrP has not been identified, no mutation near the ω site of murine PrP increased the conversion efficiency. Plausible explanations are as follows: (i) the amino acid sequence, especially near the ω site, is different among species; (ii) we examined the seed-dependent conversion in ScN2a cells but not the spontaneous conversion leading to the pathogenesis of genetic CJD. Although the GPI anchoring of human PrP with M232R has not been investigated sufficiently, a subpopulation of the mutant PrP could be GPI-anchorless and misfolded in the ER. The accumulation of these misfolded GPI-anchorless mutant PrP might lead to the spontaneous conversion. We need to further investigate the pathogenesis in animal models expressing human PrP with M232R and so on.

In conclusion, the present study shows that single amino acid substitutions near the ω site of PrP affect the GPI anchoring and the conversion efficiency. We clarified for the first time the ω site of murine PrP and the amino acid conditions near the ω site for the conversion as well as for the GPI anchoring.

Acknowledgments

We thank H. Suda for technical assistance, K. Teruya for critical advice and B. Bell for critical review of the manuscript. This study

was supported by the Promotion of Fundamental Studies in Health Science of National Institute of Biomedical Innovation (T.K.), a grant from the Ministry of Health, Labor and Welfare (A.K. and T.K.), a Grant-in-Aid for Scientific Research from the Ministry of Education, Culture, Sports, Science and Technology (A.K. and T.K.), and Grants-in-Aid from the Research Committee of Prion disease and Slow Virus Infection, the Ministry of Health, Labor and Welfare of Japan (A.K. and H.M.).

Appendix A. Supplementary data

Supplementary data associated with this article can be found, in the online version, at doi:10.1016/j.bbrc.2009.12.128.

References

[1] S.B. Prusiner, Prions, Proc. Natl. Acad. Sci. USA 95 (1998) 13363–13383.
[2] N. Stahl, D.R. Borchelt, K. Hsiao, S.B. Prusiner, Scrapie prion protein contains a phosphatidylinositol glycolipid, Cell 51 (1987) 229–240.
[3] P. Orlean, A.K. Menon, GPI anchoring of protein in yeast and mammalian cells, or: how we learned to stop worrying and love glycophospholipids, J. Lipid Res. 48 (2007) 993–1011.
[4] J. Tatzelt, K.F. Winklhofer, Folding and misfolding of the prion protein in the secretory pathway, Amyloid 11 (2004) 162–172.
[5] S. Mead, Prion disease genetics, Eur. J. Hum. Genet. 14 (2006) 273–281.
[6] T. Kitamoto, M. Ohta, K. Doh-ura, et al., Novel missense variants of prion protein in Creutzfeldt–Jakob disease or Gerstmann–Sträussler syndrome, Biochem. Biophys. Res. Commun. 191 (1993) 709–714.
[7] Y. Shiga, K. Satoh, T. Kitamoto, et al., Two different clinical phenotypes of Creutzfeldt–Jakob disease with a M232R substitution, J. Neurol. 254 (2007) 1509–1517.
[8] L. Zheng, J. Longfei, Y. Jing, et al., PRNP mutations in a series of apparently sporadic neurodegenerative dementias in China, Am. J. Med. Genet. B 147B (2008) 938–944.
[9] J. Bratosiewicz, P.P. Liberski, J. Kulczycki, R. Kordek, Codon 129 polymorphism of the PRNP gene in normal Polish population and in Creutzfeldt–Jakob disease, and the search for new mutations in PRNP gene, Acta Neurobiol. Exp. (Wars) 61 (2001) 151–156.
[10] B. Eisenhaber, P. Bork, F. Eisenhaber, Sequence properties of GPI-anchored proteins near the omega-site: constraints for the polypeptide binding site of the putative transamidase, Protein Eng. 11 (1998) 1155–1161.
[11] N. Stahl, M.A. Baldwin, A.L. Burlingame, S.B. Prusiner, Identification of glycoinositol phospholipid linked and truncated forms of the scrapie prion protein, Biochemistry 29 (1990) 8879–8884.
[12] D.R. Taylor, N.M. Hooper, The prion protein and lipid rafts, Mol. Membr. Biol. 23 (2006) 89–99.
[13] D.A. Butler, M.R. Scott, J.M. Bockman, et al., Scrapie-infected murine neuroblastoma cells produce protease-resistant prion proteins, J. Virol. 62 (1988) 1558–1564.
[14] S. Ikeda, A. Kobayashi, T. Kitamoto, Thr but Asn of the N-glycosylation sites of PrP is indispensable for its misfolding, Biochem. Biophys. Res. Commun. 369 (2008) 1195–1198.
[15] R.J. Kascsak, R. Rubenstein, P.A. Merz, et al., Mouse polyclonal and monoclonal antibody to scrapie-associated fibril proteins, J. Virol. 61 (1987) 3688–3693.
[16] M.R. Scott, R. Köhler, D. Foster, S.B. Prusiner, Chimeric prion protein expression in cultured cells and transgenic mice, Protein Sci. 1 (1992) 986–997.
[17] M. Asano, S. Mohri, J.W. Ironside, et al., vCJD prion acquires altered virulence through trans-species infection, Biochem. Biophys. Res. Commun. 342 (2006) 293–299.
[18] T. Kinoshita, M. Fujita, Y. Maeda, Biosynthesis, remodelling and functions of mammalian GPI-anchored proteins: recent progress, J. Biochem. 144 (2008) 287–294.
[19] M.E. Lowe, Site-specific mutations in the COOH-terminus of placental alkaline phosphatase: a single amino acid change converts a phosphatidylinositol-glycan-anchored protein to a secreted protein, J. Cell Biol. 116 (1992) 799–807.
[20] R. Micanovic, L.D. Gerber, J. Berger, K. Kodukula, S. Udenfriend, Selectivity of the cleavage/attachment site of phosphatidylinositol-glycan-anchored membrane proteins determined by site-specific mutagenesis at Asp-484 of placental alkaline phosphatase, Proc. Natl. Acad. Sci. USA 87 (1990) 157–161.
[21] K.F. Winklhofer, J. Heske, U. Heller, et al., Determinants of the in vivo folding of the prion protein. A bipartite function of helix 1 in folding and aggregation, J. Biol. Chem. 278 (2003) 14961–14970.
[22] B. Chesebro, M. Trifilo, R. Race, et al., Anchorless prion protein results in infectious amyloid disease without clinical scrapie, Science 308 (2005) 1435–1439.
[23] S. Kiachopoulos, A. Bracher, K.F. Winklhofer, J. Tatzelt, Pathogenic mutations located in the hydrophobic core of the prion protein interfere with folding and attachment of the glycosylphosphatidylinositol anchor, J. Biol. Chem. 280 (2005) 9320–9329.
[24] M.C. Field, P. Moran, W. Li, G.A. Keller, I.W. Caras, Retention and degradation of proteins containing an uncleaved glycosylphosphatidylinositol signal, J. Biol. Chem. 269 (1994) 10830–10837.
[25] K. Nakatsukasa, J.L. Brodsky, The recognition and retrotranslocation of misfolded proteins from the endoplasmic reticulum, Traffic 9 (2008) 861–870.
[26] S.W. Kang, N.S. Rane, S.J. Kim, et al., Substrate-specific translocational attenuation during ER stress defines a pre-emptive quality control pathway, Cell 127 (2006) 999–1013.

J. Comp. Path. 2010, Vol. ■, 1–6

Available online at www.sciencedirect.com

ScienceDirect

ELSEVIER

www.elsevier.com/locate/jcpa

Antigen Retrieval Using Sodium Hydroxide for Prion Immunohistochemistry in Bovine Spongiform Encephalopathy and Scrapie

H. Okada*, Y. Sato†, T. Sata†, M. Sakurai*, J. Endo*, T. Yokoyama* and S. Mohri*

** Prion Disease Research Team, Prion Disease Research Center, National Institute of Animal Health, 3-1-5 Kan-nondai, Tsukuba, Ibaraki 305-0856 and † Department of Pathology, National Institute of Infectious Diseases, 1-23-1 Toyama, Shinjuku, Tokyo 162-8640, Japan*

Summary

Formalin-fixed and paraffin wax-embedded (FFPE) tissue sections are usually used for histopathological and immunohistochemical analyses in prion diseases in animals and man. However, formalin fixation cross-links proteins, reducing disease-associated prion protein (PrP^{Sc}) immunolabelling. To detect PrP^{Sc} in animals naturally affected with bovine spongiform encephalopathy (BSE) and scrapie, we applied minimal pretreatment with sodium hydroxide (NaOH). This simple pretreatment, combined with enzymatic digestion using proteinase K (PK), was equally effective in the detection of PrP^{Sc} in FFPE tissue, and superior in terms of speed, compared with the usual autoclaving method. The most effective results, without any section loss, were obtained with 10 μg/ml PK in phosphate buffered saline containing 0.1% Triton-X at room temperature for 10 min and 150 mM NaOH at 60°C for 10 min. By this simple procedure, PrP^{Sc} was visualized in the brain of animals with BSE and scrapie using a range of anti-PrP primary antibodies.

Keywords: antigen retrieval; BSE; immunohistochemistry; scrapie

Introduction

Transmissible spongiform encephalopathy (TSE), also known as prion disease, is a neurodegenerative disorder characterized by the presence of an abnormal, protease-resistant isoform of prion protein (PrP^{Sc}) (Prusiner *et al.*, 1982). Enzyme-linked immunosorbent assay, western blotting and immunohistochemistry (IHC) are used for the diagnosis of TSEs such as scrapie in sheep and goats, bovine spongiform encephalopathy (BSE) in cattle, chronic wasting disease (CWD) in deer and Creutzfeldt–Jacob disease (CJD) and Gerstmann–Sträussler–Scheinker syndrome (GSS) in man. Formalin-fixed specimens of brain are conventionally used for histopathological and immunohistochemical diagnosis of TSEs (Bodemer, 1999).

Formalin fixation cross-links proteins; therefore, antigen retrieval protocols are often needed for formalin-fixed tissue samples (Pollock and Wood, 1988). Pretreatments, such as chemical, high-temperature, enzymatic and combined treatments, for various times are required for the immunohistochemical detection of disease-associated PrP^{Sc}; these pretreatments induce the denaturation of conformational changes in formalin-fixed tissue proteins (Van Everbroeck *et al.*, 1999; Privat *et al.*, 2000). Chemical pretreatment, consisting of baths of potassium permanganate, sodium disulphite and sodium hydroxide (NaOH), was recently reported to be effective for the detection of immunolabelled PrP^{Sc} in formalin-fixed paraffin wax-embedded (FFPE) tissues from cattle with BSE (Bencsik *et al.*, 2005). The aim of this study was to evaluate the effect of simple chemical pretreatment, consisting of proteinase K (PK) digestion (10 mg/ml for 10 min at

Correspondence to: H. Okada (e-mail: okadahi@affrc.go.jp).

0021-9975/$ - see front matter
doi:10.1016/j.jcpa.2010.10.001

Please cite this article in press as: Okada H et al., Antigen Retrieval Using Sodium Hydroxide for Prion Immunohistochemistry in Bovine Spongiform Encephalopathy and Scrapie, Journal of Comparative Pathology (2010), doi:10.1016/j.jcpa.2010.10.001

room temperature [RT]) followed by a bath of 150 mM NaOH (10 min at 60°C), for specific PrP^{Sc} immunolabelling in FFPE sections from animals naturally affected with BSE and scrapie.

Materials and Methods

Samples

The medulla oblongata at the obex level of five cattle with naturally occurring BSE (BSE/JP17, 21, 22, 35, 36) and one sheep with naturally occurring scrapie (domestic case from Kanagawa in 2005) was removed from the heads and fixed in 10% neutral buffered formalin. Formalin-fixed brainstem samples were sent to our laboratory. Coronal slices of the samples were cut and immersed in 98% formic acid for 60 min at RT to reduce infectivity (Taylor *et al.*, 1997) and then embedded in paraffin wax. Sections (4 μm) were mounted on silane-coated glass slides (Immuno-Coat, Muto Pure Chemicals, Tokyo, Japan), stained with haematoxylin and eosin (HE) or subjected to immunohistochemical analysis. Brains of two BSE-negative cattle and two scrapie-negative sheep were used as controls.

Pretreatment

Dewaxed sections were treated with 3% H_2O_2 for 10 min at RT followed by incubation with or without 10 μg/ml PK in phosphate buffered saline (pH 7.4, 0.01 M) containing 0.1% Triton-X (PBST) for 10 min at RT. For the development of the optimal protocol, sections were subsequently soaked in NaOH corresponding to 0, 50, 100, 150 and 300 mM. Treatment with each concentration of NaOH was undertaken for 10 min at RT, 37°C and 60°C, respectively.

To ensure the sensitivity and specificity of PrP^{Sc} immunolabelling, after these pretreatments the sections were autoclaved for 3 min at 121°C in 10 mM citrate buffer (pH 6.0).

Immunohistochemistry

IHC was performed in automated fashion (DakoCytomation Autostainer Universal Staining System, Dako, Carpinteria, California) at RT. After applying each step, sections were rinsed in tap water for 5 min and briefly rinsed in PBST. Sections were incubated first with 10% normal goat serum (Sigma, St Louis, Missouri) for 10 min and then with anti-PrP primary monoclonal (mAb) or polyclonal antibody (pAb) for 60 min. The third stage of the procedure was incubation with anti-mouse or anti-rabbit universal immunoperoxidase polymer (Nichirei Histofine Simple Stain MAX-PO [M] or [R], Nichirei, Tokyo, Japan) as secondary antibody for 30 min. Labelling was 'visualized' by incubation with 3′,3-diaminobenzidine tetrachloride as chromogen for 7 min. Sections were counterstained with haematoxylin.

Test Battery

Initially, a test battery was employed to develop an optimal protocol using mAb SAF84 (1 μg/ml, SPI-bio, Montigny le Bretonneux, France) based on a previous report (Bencsik *et al.*, 2005). After the optimal protocol was derived, nine antibodies were used to demonstrate PrP^{Sc} immunolabelling. The characteristics of the 10 primary antibodies used in this study are summarized in Table 1.

Table 1
Characteristics of the antibodies used in this study

Antibody	*Epitope location*	*PrP sequence numbering*	*Dilution*	*Clonality*	*Immunogen*	*Source*
SAF32	Octa-repeat region		1 μg/ml	Monoclonal	SAF from infected hamster brain	SPI-bio, Montigny le Bretonneux, France
B103	103–121	Cattle	1 in 100	Polyclonal	Cattle recPrP	FUJIREBIO, Tokyo, Japan
12F10	142–160	Human	1 μg/ml	Monoclonal	Hamster recPrP	SPI-bio
SAF54	142–160	Human	1 μg/ml	Monoclonal	SAF from infected hamster brain	SPI-bio
F89/160.1.5	146–159	Cattle	1 μg/ml	Monoclonal	Cattle recPrP	VMRD, Pullman, Washington
44B1	155–231	Mouse	1 μg/ml	Monoclonal	Mouse recPrP	Dr. Horiuchi (Kim *et al.*, 2004)
SAF84	160–170	Human	1 μg/ml	Monoclonal	SAF from infected hamster brain	SPI-bio
43C5	163–169	Mouse	1 μg/ml	Monoclonal	Mouse recPrP	Dr. Horiuchi (Kim *et al.*, 2004)
T4	221–239	Cattle	1 in 100	Polyclonal	Cattle recPrP	Dr. Sata (Takahashi *et al.*, 1999)
F99/97.6.1	228–233	Cattle	1 μg/ml	Monoclonal	Cattle recPrP	VMRD

Please cite this article in press as: Okada H et al., Antigen Retrieval Using Sodium Hydroxide for Prion Immunohistochemistry in Bovine Spongiform Encephalopathy and Scrapie, Journal of Comparative Pathology (2010), doi:10.1016/j.jcpa.2010.10.001

Results

The intensity of PrP^{Sc} immunolabelling increased in a concentration- and temperature-dependent manner in both BSE and scrapie specimens pretreated with NaOH using mAb SAF84 (Figs. 1, 2; Table 2). Additional enzymatic digestion with PK significantly enhanced the intensity of PrP^{Sc} immunolabelling in both BSE and scrapie samples. Simple NaOH pretreatment with additional PK digestion was equally effective in visualizing PrP^{Sc} immunolabelling with less non-specific background compared with the usual autoclaving method tested here, which was devoid of immunolabelling reduction and section loss from glass slides (Figs. 1–3). Sections incubated in 150 mM and 300 mM NaOH at 60°C showed striking immunolabelling and no significant difference in the intensity of PrP^{Sc} immunolabelling in most cases. Notably, various types of PrP^{Sc} deposition (i.e. granular, linear, coalescing, intraneuronal, perineuronal and intraglial) were detected in both BSE and scrapie samples using simple chemical pretreatment. No obvious difference was present in PrP^{Sc} labelling patterns and immunolabelling intensity between simple chemical pretreatment and autoclaving.

To compare the intensity of PrP^{Sc} immunolabelling using the other nine primary antibodies, simple chemical pretreatment was performed with 150 mM NaOH at 60°C with PK digestion. All antibodies used in this study reacted with both bovine and ovine PrP^{Sc} (Table 3). However, the intensity of PrP^{Sc} immunolabelling varied with the two pretreatment methods. Moderate to intense PrP^{Sc} labelling was detected with simple chemical pretreatment in both BSE and scrapie samples using mAbs SAF54, F89/160.1.5, F99/97.6.1, 43C5 and 44B1(Kim *et al.*, 2004), and pAb T4 (Takahashi *et al.*, 1999). However, the immunolabelling intensity of PrP^{Sc} under simple chemical pretreatment was weak using some antibodies (mAb SAF32 and pAb B103) that recognised the N-terminal epitope region in comparison with the results obtained from the autoclaving pretreatment. Moreover, weak immunolabelling was detected in a scrapie brain, using mAb 12F10. No specific immunolabelling against PrP^{Sc} was detected in control animals by using either the usual autoclaving or simple chemical pretreatments.

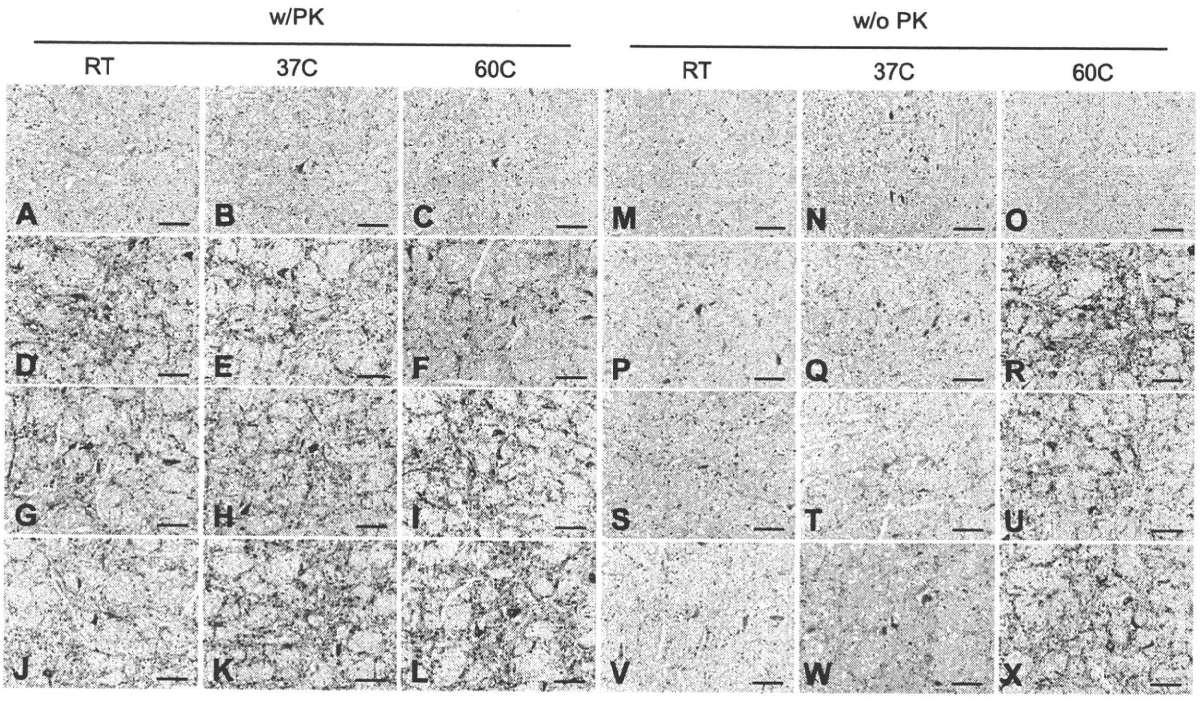

Fig. 1. Comparison of PrP^{Sc} immunolabelling intensity in sections treated with different concentrations of NaOH and different incubation temperatures. Sections are derived from the reticular formation of the medulla oblongata at the level of the obex from cattle with BSE (BSE/JP36). The experiment was performed with the test battery using mAb SAF84 and pretreated with (A–L) or without (M–X) PK digestion. First row, no NaOH treatment (A–C, M–O); second row, treated with 50 mM NaOH (D–F, P–R); third row, treated with 150 mM NaOH (G–I, S–U); bottom row, treated with 300 mM NaOH (J–L, V–X). Each pretreatment was for 10 min. Bar, 50 μm.

Please cite this article in press as: Okada H et al., Antigen Retrieval Using Sodium Hydroxide for Prion Immunohistochemistry in Bovine Spongiform Encephalopathy and Scrapie, Journal of Comparative Pathology (2010), doi:10.1016/j.jcpa.2010.10.001

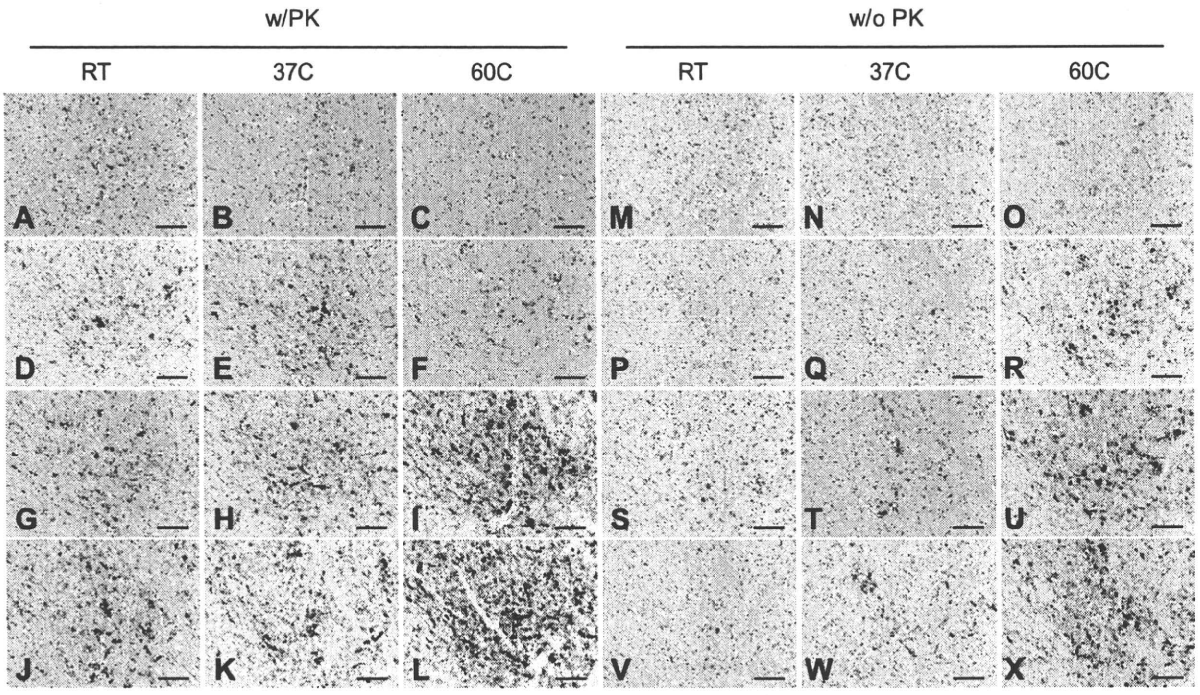

Fig. 2. Effects of NaOH concentration and treatment temperature on PrP^{Sc} immunolabelling in the spinal trigeminal nucleus of the medulla oblongata at the level of the obex of sheep with scrapie. Analysis was performed with the test battery using mAb SAF84 pretreated with (A–L) or without (M–X) PK digestion. First row, no NaOH treatment (A–C, M–O); second row, treated with 50 mM NaOH (D–F, P–R); third row, treated with 150 mM NaOH (G–I, S–U); bottom row, treated with 300 mM NaOH (J–L, V–X). Each pretreatment was for 10 min. Bar, 50 μm.

Discussion

The results of this study provide convincing evidence that a simple chemical pretreatment might be a reliable antigen retrieval technique for the immunohistochemical demonstration of bovine and ovine PrP^{Sc}. Formalin-fixed specimens are conventionally used for histopathological and immunohistochemical diagnosis of TSEs (Bodemer, 1999). However, formalin fixation cross-links proteins; therefore, antigen retrieval protocols are often required (Pollock and Wood, 1988). Appropriate antigen retrieval is essential to unmask the PrP^{Sc} epitope and diminish PrP^{C} in FFPE tissue sections with prion diseases (Van Everbroeck *et al.*, 1999). Several antigen retrieval procedures, such as a combination of chemical, high-temperature and enzymatic pretreatments, have been applied for the detection of PrP^{Sc} by different researchers (Kitamoto *et al.*, 1987; Haritani *et al.*, 1994; Van Everbroeck *et al.*, 1999; Privat *et al.*, 2000; Furuoka *et al.*, 2005).

Table 2
Intensity of PrP^{sc} immunolabelling detected by mAb SAF84 following different treatments

NaOH concentration (mM)	*With PK digestion*			*Without PK digestion*		
	RT	*37°C*	*60°C*	*RT*	*37°C*	*60°C*
0	±	+	+	±	+	+
50	2+	2+	2+	+	+	2+
100	2+	2+	2+	+	+	2+
150	2+	2+	3+	+	+	2+
300	2+	2+	3+	+	+	2+

Immunolabelling intensity: ±, sparse; +, weak; 2+, distinct; 3+, strong.
RT, room temperature.

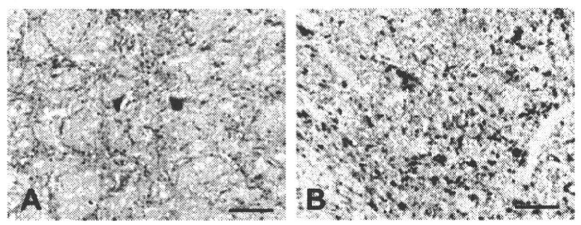

Fig. 3. Immunohistochemical detection of bovine and ovine PrP^{Sc} in (A) the reticular formation of the medulla oblongata of a BSE-affected cow (BSE/JP36) and (B) the spinal trigeminal nucleus of the medulla oblongata of a scrapie-affected sheep. Usual autoclaving pretreatment using mAb SAF84 was applied. Bar, 50 μm.

Please cite this article in press as: Okada H et al., Antigen Retrieval Using Sodium Hydroxide for Prion Immunohistochemistry in Bovine Spongiform Encephalopathy and Scrapie, Journal of Comparative Pathology (2010), doi:10.1016/j.jcpa.2010.10.001

Table 3
Immunolabelling intensity with 10 antibodies under two different pretreatments

Antibody	*BSE*		*Scrapie*	
	AC	*NaOH*	*AC*	*NaOH*
SAF32	2+	+	2+	+
B103	2+	+	2+	+
12F10	2+	3+	+	±
SAF54	2+	2+	2+	2+
F89/160.1.5	3+	3+	3+	2+
SAF84	3+	3+	3+	3+
43C5	2+	3+	3+	3+
44B1	2+	3+	3+	3+
T4	2+	3+	2+	2+
F99/97.6.1	3+	3+	3+	3+

Immunolabelling intensity: ±, sparse; +, weak; 2+, distinct; 3+, strong.
AC, autoclaving in 10 mM citrate buffer (pH 6.0) at 121°C for 3 min; NaOH, treated with 150 mM NaOH at 60°C for 10 min.

Strong alkaline or high-temperature treatment modifies the protein structure, as shown by formalin fixation (Shi *et al.*, 1997, 2001). Although the mechanism of antigen retrieval in PrP^{Sc} IHC using alkaline chemicals is unclear, hydrolysis that results from strong alkaline treatment may be a critical factor (Shi *et al.*, 1997, 2001). Hydrated or hydrolytic autoclave pretreatment for the enhancement of PrP^{Sc} immunolabelling appears necessary to unmask protein cross-linkage (Haritani *et al.*, 1994). Autoclaving in citrate buffer (pH 6.0) enhances demonstration of immunolabelled PrP^{Sc} in BSE tissue (Terry *et al.*, 2003), suggesting that citrate may be effective in inducing calcium chelation (Morgan *et al.*, 1994; Shi *et al.*, 1997, 2001).

The results of the present study also demonstrate that PK digestion followed by NaOH pretreatment can effectively enhance PrP^{Sc} immunolabelling in BSE and scrapie samples. PK pretreatment has been reported to be efficient for the amplification of PrP^{Sc} immunolabelling in BSE (Brun *et al.*, 2004) and CJD specimens (Privat *et al.*, 2000). In contrast, enzymatic digestion with PK, alone or combined with chemical pretreatments such as with formic acid or guanidine thiocyanate, did not increase PrP^{Sc} immunolabelling (Hayward *et al.*, 1994). The discrepancy in these results might be due to the different technical protocols applied.

The present chemical pretreatment did not cause section loss from slides despite treatment with 300 mM NaOH. However, the simple chemical method was not effective with every PrP antibody and in every species, but it was also efficient in deer affected with CWD and in mice experimentally affected with TSEs such as classical BSE, scrapie and GSS (data not shown). We were also able to detect very weak or no PrP^{Sc} immunolabelling in samples treated with the simple chemical method (Bencsik *et al.*, 2005) when using mAbs SAF32 and 12F10 utilized for immunohistochemical analysis of TSE samples (data not shown).

In summary, this investigation has shown that simple chemical pretreatment based on NaOH combined with PK digestion yields strong PrP^{Sc} immunolabelling in tissues from animals with BSE and scrapie, and may be utilized with many antibodies in TSE immunohistochemical studies.

Acknowledgments

We thank Dr. Y. Tagawa (National Institute of Animal Health) for providing anti-prion mAb T1 and Dr. M. Horiuchi (Graduate School of Veterinary Medicine, Hokkaido University) for providing mAbs 44B1 and 43C5. The authors are very grateful to Ms. N. Amagai and M. Kakizaki (National Institute of Animal Health) for their expert technical assistance. This work was supported by grants from the BSE and other Prion Disease Control Project of the Ministry of Agriculture, Forestry and Fisheries of Japan and from the BSE Research Project of the Ministry of Health, Labor and Welfare of Japan.

References

Bencsik AA, Debeer SO, Baron TG (2005) An alternative pretreatment procedure in animal transmissible spongiform encephalopathies diagnosis using PrPsc immunohistochemistry. *Journal of Histochemistry and Cytochemistry*, **53**, 1199–1202.

Bodemer W (1999) The use of monoclonal antibodies in human prion disease. *Naturwissenschaften*, **86**, 212–220.

Brun A, Castilla J, Ramirez MA, Prager K, Parra B *et al.* (2004) Proteinase K enhanced immunoreactivity of the prion protein-specific monoclonal antibody 2A11. *Neuroscience Research*, **48**, 75–83.

Furuoka H, Yabuzoe A, Horiuchi M, Tagawa Y, Yokoyama T *et al.* (2005) Effective antigen-retrieval method for immunohistochemical detection of abnormal isoform of prion proteins in animals. *Acta Neuropathologica (Berlin)*, **109**, 263–271.

Haritani M, Spencer YI, Wells GA (1994) Hydrated autoclave pretreatment enhancement of prion protein immunoreactivity in formalin-fixed bovine spongiform encephalopathy-affected brain. *Acta Neuropathologica (Berlin)*, **87**, 86–90.

Hayward PA, Bell JE, Ironside JW (1994) Prion protein immunocytochemistry: reliable protocols for the investigation of Creutzfeldt–Jakob disease. *Neuropathology and Applied Neurobiology*, **20**, 375–383.

Kim CL, Karino A, Ishiguro N, Shinagawa M, Sato M *et al.* (2004) Cell-surface retention of PrP^{C} by anti-PrP

Please cite this article in press as: Okada H et al., Antigen Retrieval Using Sodium Hydroxide for Prion Immunohistochemistry in Bovine Spongiform Encephalopathy and Scrapie, Journal of Comparative Pathology (2010), doi:10.1016/j.jcpa.2010.10.001

antibody prevents protease-resistant PrP formation. *Journal of General Virology*, **85**, 3473–3482.

Kitamoto T, Ogomori K, Tateishi J, Prusiner SB (1987) Formic acid pretreatment enhances immunostaining of cerebral and systemic amyloids. *Laboratory Investigation*, **57**, 230–236.

Morgan JM, Navabi H, Schmid KW, Jasani B (1994) Possible role of tissue-bound calcium ions in citrate-mediated high-temperature antigen retrieval. *Journal of Pathology*, **174**, 301–307.

Pollock NJ, Wood JG (1988) Differential sensitivity of the microtubule-associated protein, tau, in Alzheimer's disease tissue to formalin fixation. *Journal of Histochemistry and Cytochemistry*, **36**, 1117–1121.

Privat N, Sazdovitch V, Seilhean D, LaPlanche JL, Hauw JJ (2000) PrP immunohistochemistry: different protocols, including a procedure for long formalin fixation, and a proposed schematic classification for deposits in sporadic Creutzfeldt–Jakob disease. *Microscience Research Techniques*, **50**, 26–31.

Prusiner SB, Bolton DC, Groth DF, Bowman KA, Cochran SP *et al.* (1982) Further purification and characterization of scrapie prions. *Biochemistry*, **21**, 6942–6950.

Shi SR, Cote RJ, Taylor CR (1997) Antigen retrieval immunohistochemistry: past, present, and future. *Journal of Histochemistry and Cytochemistry*, **45**, 327–343.

Shi SR, Cote RJ, Taylor CR (2001) Antigen retrieval techniques: current perspectives. *Journal of Histochemistry and Cytochemistry*, **49**, 931–937.

Takahashi H, Takahashi RH, Hasegawa H, Horiuchi M, Shinagawa M *et al.* (1999) Characterization of antibodies raised against bovine-PrP-peptides. *Journal of Neurovirology*, **5**, 300–307.

Taylor DM, Brown JM, Fernie K, McConnell I (1997) The effect of formic acid on BSE and scrapie infectivity in fixed and unfixed brain-tissue. *Veterinary Microbiology*, **58**, 167–174.

Terry LA, Marsh S, Ryder SJ, Hawkins SA, Wells GA *et al.* (2003) Detection of disease-specific PrP in the distal ileum of cattle exposed orally to the agent of bovine spongiform encephalopathy. *Veterinary Record*, **152**, 387–392.

Van Everbroeck B, Pals P, Martin JJ, Cras P (1999) Antigen retrieval in prion protein immunohistochemistry. *Journal of Histochemistry and Cytochemistry*, **47**, 1465–1470.

[*Received, May 17th, 2010*
Accepted, October 18th, 2010]

Please cite this article in press as: Okada H et al., Antigen Retrieval Using Sodium Hydroxide for Prion Immunohistochemistry in Bovine Spongiform Encephalopathy and Scrapie, Journal of Comparative Pathology (2010), doi:10.1016/j.jcpa.2010.10.001

nature medicine

Ultrasensitive human prion detection in cerebrospinal fluid by real-time quaking-induced conversion

Ryuichiro Atarashi[1,2], Katsuya Satoh[1], Kazunori Sano[1,3], Takayuki Fuse[1], Naohiro Yamaguchi[1], Daisuke Ishibashi[1], Takehiro Matsubara[1], Takehiro Nakagaki[1], Hitoki Yamanaka[4], Susumu Shirabe[5], Masahito Yamada[6], Hidehiro Mizusawa[7], Tetsuyuki Kitamoto[8], Genevieve Klug[9], Amelia McGlade[9], Steven J Collins[9] & Noriyuki Nishida[1,3]

The development of technologies for the *in vitro* amplification of abnormal conformations of prion protein (PrP^{Sc}) has generated the potential for sensitive detection of prions. Here we developed a new PrP^{Sc} amplification assay, called real-time quaking-induced conversion (RT-QUIC), which allows the detection of ≥1 fg of PrP^{Sc} in diluted Creutzfeldt-Jakob disease (CJD) brain homogenate. Moreover, we assessed the technique first in a series of Japanese subjects and then in a blind study of 30 cerebrospinal fluid specimens from Australia, which achieved greater than 80% sensitivity and 100% specificity. These findings indicate the promising enhanced diagnostic capacity of RT-QUIC in the antemortem evaluation of suspected CJD.

Transmissible spongiform encephalopathies, or prion diseases, are characteristically associated with the accumulation of PrP^{Sc} in the central nervous system through autocatalytic conversion of normal cellular PrP (PrP^{C}) into replicate misfolded isomers[1,2]. Despite a few other reported markers[3,4], PrP^{Sc} remains the best characterized and most reliable marker of prion disease.

Definitive antemortem confirmation of CJD requires the detection of PrP^{Sc} in biopsy specimens, the practice of which is discouraged because it is invasive and poses risks to health care personnel. Recently, however, *in vitro* PrP^{Sc} amplification techniques, including protein misfolding cyclic amplification[5–7], the amyloid seeding assay[8] and QUIC, have been reported to enable the direct and highly sensitive detection of PrP^{Sc} in various tissues, including cerebrospinal fluid (CSF). QUIC assays involve the use of soluble recombinant PrP (rPrP-sen) as a substrate, which is seeded with PrP^{Sc} and then subjected to intermittent automated shaking. This technique can be performed more easily than the protein misfolding cyclic amplification, which requires repeated sonication. Previous studies have shown that QUIC assays correctly discriminate between normal and scrapie-infected CSF samples in both hamster and sheep prion disease models[9,10]. However, ultrasensitive PrP^{Sc} detection in CSF from subjects with CJD has not yet been accomplished. Accordingly, we further refined the QUIC assay to improve its sensitivity and practicability and then applied the technique in a blind pilot study to detect PrP^{Sc} in CJD CSF specimens.

Given that a correlation between protease-resistant rPrP aggregate (rPrP-res) abundance and thioflavin T (ThT) fluorescence had been shown previously[7], we sought to determine the relative kinetics of rPrP-res formation by monitoring levels of ThT fluorescence in the QUIC assay. This was intended to minimize the time needed to detect rPrP-res. We first tested whether PrP^{Sc}-dependent rPrP-res ($rPrP\text{-}res^{Sc}$) formation could be induced in a microplate reader with intermittent shaking. We used human rPrP-sen (rHuPrP-sen) and a 10^{-7} dilution of CJD (molecular subtype MM1) brain homogenate as the substrate and seed, respectively. We conducted QUIC reactions at various concentrations (0, 0.25, 0.5 and 1.0 M) of guanidine-HCl (GdnHCl), because it has been shown that GdnHCl greatly enhances conversion of PrP-sen to PrP-res in cell-free conversion reactions[11]. Unexpectedly, we observed positive PrP^{Sc}-dependent ThT fluorescence within 24 h, both in the presence and in the absence of GdnHCl (**Fig. 1a**). In contrast, the negative control reactions without seed and in the absence of GdnHCl resulted in no increase in ThT fluorescence over 24 h; however, *de novo* formation of rPrP-res ($rPrP\text{-}res^{spon}$) was rapidly induced in the presence of GdnHCl when shaking was added (**Fig. 1a,b**). These results indicate that shaking accelerates PrP^{Sc}-dependent $rPrP\text{-}res^{Sc}$ formation even without GdnHCl (**Supplementary Fig. 1**), albeit with a lower peak of fluorescence.

Shaking is thought to cause partial unfolding of a portion of rPrP-sen by increasing the air-water interface[12]. Moreover, shaking enhances the interaction between rPrP-sen and PrP^{Sc} and promotes the fragmentation of rPrP-res polymers[13]. It is generally accepted that the energetic barrier of seed-dependent fibril formation and elongation is lower than that of spontaneous fibril formation, which first requires nucleation as the rate-limiting step[14]. The partial unfolding of rPrP-sen by shaking seems to be more heterogeneous than that facilitated by a denaturant such as GdnHCl, perhaps because the air-water interfaces created by shaking are unequally distributed

[1]Department of Molecular Microbiology and Immunology, Nagasaki University Graduate School of Biomedical Sciences, Nagasaki, Japan. [2]Nagasaki University Research Centre for Genomic Instability and Carcinogenesis, Nagasaki, Japan. [3]Global Centers of Excellence Program, Nagasaki University, Nagasaki, Japan. [4]Division of Comparative Medicine, Center for Frontier Life Sciences, Nagasaki University, Nagasaki, Japan. [5]Organization of Rural Medicine and Residency Education, Nagasaki University Hospital, Nagasaki, Japan. [6]Department of Neurology and Neurobiology of Aging, Kanazawa University Graduate School of Medical Science, Kanazawa, Japan. [7]Department of Neurology and Neurological Science, Graduate School, Tokyo Medical and Dental University, Tokyo, Japan. [8]Division of Creutzfeldt-Jakob Disease Science and Technology, Department of Prion Research, Tohoku University Graduate School of Medicine, Sendai, Japan. [9]Department of Pathology, Australian National Creutzfeldt-Jakob Disease Registry, University of Melbourne, Melbourne, Australia. Correspondence should be addressed to R.A. (atarashi@nagasaki-u.ac.jp).

Received 2 July 2010; accepted 16 December 2010; published online 30 January 2011; doi:10.1038/nm.2294

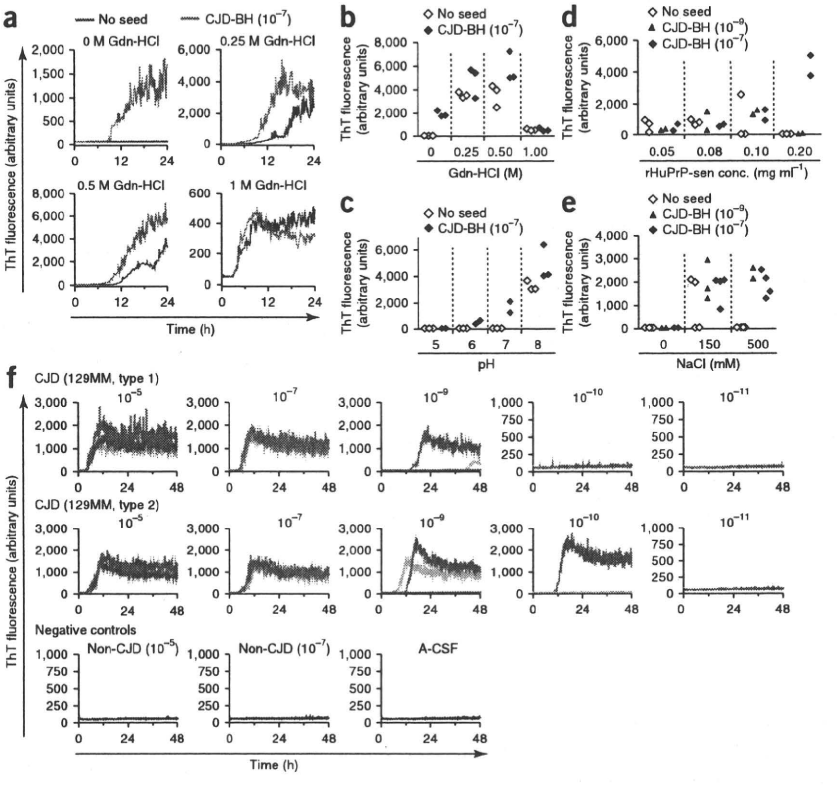

Figure 1 QUIC reactions induce PrP^{Sc}-dependent rHuPrP-res formation under GdnHCl-free conditions. (**a**,**b**) The effect of the indicated concentration of Gdn-HCl on the kinetics of rHuPrP fibril formation with or without 10^{-7} dilution of CJD brain homogenate (CJD-BH) (type 1, 129MM). The reaction buffer contained 150 mM NaCl, 50 mM PIPES, pH 7.0, 1 mM EDTA and 10 μM ThT. The concentration of rHuPrP-sen was 0.1 mg ml^{-1}. The graphs in **a** depict one representative of triplicates. The maximal fluorescence intensity of each single reaction for 24 h is plotted in **b**. (**c**–**e**) The effect of pH (**c**), the concentration of rHuPrP-sen (**d**) and the concentration of NaCl (**e**) were tested with the indicated dilutions of CJD-BH (type 1, 129MM) as seeds. Buffers used in **c** were pH 5 50 mM sodium acetate buffer, pH 6 50 mM MES, pH 7 50 mM PIPES and pH 8 50 mM HEPES. The concentration of NaCl in **c** and **d** was 150 mM, the pH of the buffer in **d** and **e** was 7.0 (50 mM PIPES) and the rHuPrP-sen concentration in **c** and **e** was 0.1 mg ml^{-1}. Each symbol represents the maximal fluorescence intensity from an individual reaction for 48 h. (**f**) Detection limit of RT-QUIC with the indicated dilutions of CJD-BH (129MM, type 1) and CJD-BH (129MM, type 2) as seeds. We used the indicated dilutions of non–CJD-BH (dissecting aneurysm) or artificial CSF (A-CSF) as negative controls. We performed the RT-QUIC reactions as described in the **Supplementary Methods**. The colored curves represent the kinetics of ThT fluorescence from an individual reaction seeded with the same dilution of BH. The graphs are representative of two independent experiments, each performed in triplicate.

in solution. We found that the addition of GdnHCl to QUIC reactions leads to an increase in the nucleation rate, and increased spontaneous fibril formation. The early appearance of rPrP-res^{spon} decreases the specificity of QUIC, because ThT fluorescence cannot distinguish between rPrP-res^{Sc} and rPrP-res^{spon}. Therefore, we chose not to use GdnHCl in subsequent analyses.

To further optimize the conditions, we examined the effects of pH, as well as of the concentrations of rHuPrP-sen and salt on QUIC reactions in GdnHCl-free conditions with shaking (**Fig. 1c–e** and **Supplementary Fig. 2**). After assessment, we successfully established a method for the real-time monitoring of the kinetics of rPrP fibril formation seeded with CJD brain homogenate (see **Supplementary Methods**), without the generation of rPrP-res^{spon} and designated the assay RT-QUIC.

To determine the minimum amount of PrP^{Sc} detectable by RT-QUIC, we diluted CJD brain homogenate (MM1 and MM2) serially with artificial CSF (A-CSF) and used these dilutions to seed the reactions. We observed increased PrP^{Sc}-dependent ThT fluorescence within 48 h in more than half the replicates of CJD brain homogenate, with dilutions ranging from 10^{-5} to 10^{-9} (**Fig. 1f** and **Supplementary Table 1**). With 10^{-10} brain homogenate dilutions, we observed a marginally lower rate of positive reactions, and 10^{-11} dilutions of the CJD-brain homogenates produced no ThT fluorescence response (**Fig. 1f** and **Supplementary Table 1**). The negative controls seeded with 10^{-5} and 10^{-7} dilutions of non-CJD brain homogenate or A-CSF alone (no seed) did not produce an increase in the fluorescence (**Fig. 1f** and **Supplementary Table 1**). The 10^{-9} dilutions of MM1 and MM2 CJD brain homogenate contained approximately 0.8 and 1.9 fg of PrP^{Sc}, respectively, according to our estimation (data not shown). Consequently, the results indicate that this assay consistently enables us to detect more than or equal to about 1 fg of PrP^{Sc} in the diluted CJD brain homogenates within 48 h. Moreover, the fact that there was no rPrP-res^{spon} formation under the conditions used implies a lower and acceptable risk of false-positive reactions. Whether the RT-QUIC has the same sensitivity to CJD brain homogenate with 129MV or 129VV as 129MM remains to be determined.

CSF is routinely used in the evaluation of central nervous system disorders and presumably contains more PrP^{Sc} and fewer impurities than blood. This prompted us to compare the RT-QUIC seeding activity in CSF samples from subjects with CJD and subjects without CJD but with other neurodegenerative diseases. For the pilot study, we initially tested CJD CSF samples from 18 definite cases of CJD in Japan (**Table 1**) and 35 non-CJD controls from subjects with other neurodegenerative diseases (**Supplementary Table 2**). We saw a minimal ThT fluorescence increase in the controls, with no false positives in the assay. In contrast, increased PrP^{Sc}-dependent fluorescence was seen in at least one of four replicates in 15/18 (83.3%) of the CJD CSF samples (**Table 1** and **Supplementary Table 3**).

To further confirm the reliability of RT-QUIC, we conducted a blind trial using 30 CSF samples from the Australian National CJD Registry and 155 CSF samples containing 25 probable cases of CJD and 130 cases of other neurological diseases obtained in Japan. In the Australian samples, we were able to detect PrP^{Sc} in 14/16 (87.5%) definite CJD CSF samples, as opposed to 0/14 of the non-CJD controls (**Table 1**, **Supplementary Fig. 3** and **Supplementary Table 3**). It should be noted that 3/4 129VV and 2/2 129MV cases were positive by RT-QUIC.

Table 1 Clinical data and RT-QUIC reactions seeded with CSF samples

CSF from 18 definite CJD samples in Japan					
Sample	Age (years)/sex	CJD type	Molecular subtype[a]	14-3-3 (γ-isoform)[b]	RT- QUIC[c]
C1	68/M	sCJD	MM 1	+	+ (3/4)
C2	66/F	sCJD	MM 1	+	+ (2/4)
C3	71/F	sCJD	MM 1	+	+ (1/4)
C4	57/F	sCJD	MM 2	+	+ (2/4)
C5	70/M	sCJD	MM 2	+	+ (2/4)
C6	66/M	sCJD	MM 2	+	+ (2/4)
C7	60/F	sCJD	MM 2	–	– (0/4)
C8	73/F	sCJD	MM 2	+	+ (4/4)
C9	74/M	sCJD	MM 2	+	– (0/4)
C10	79/F	sCJD	MM 2	–	+ (3/4)
C11	65/F	sCJD	MM 2	+	+ (4/4)
C12	69/M	sCJD	MM 2	+	– (0/4)
C13	69/F	sCJD	MM 2	+	+ (3/4)
C14	54/F	sCJD	MM 2	+	+ (3/4)
C15	76/F	sCJD	MM 2	–	+ (2/4)
C16	68/M	sCJD	MM 2	–	+ (4/4)
C17	58/F	iCJD	MM 1	+	+ (3/4)
C18	79/F	iCJD	MM 1	–	+ (3/4)

Blind trial of 30 CSF samples in Australia						
Sample	Age (years)/sex	Diagnosis[d]	Codon 129	Profile of PrP^{Sc}	14-3-3 (all isoforms)[e]	RT-QUIC[g]
A1	53/F	PN/MC			–	– (0/4)
A2	59/F	PN/ MC			–	– (0/4)
A3	85/M	AD			–	– (0/4)
A4	60/F	ICD			+	– (0/4)
A5	83/M	AD			+	– (0/4)
A6	73/M	sCJD	VV	2	+	+ (2/4)
A7	67/F	sCJD	MM	1	+	+ (4/4)
A8	82/F	sCJD	MM	1	+	+ (2/4)
A9	67/M	sCJD	MV	1	–	+ (2/4)
A10	50/M	sCJD	MM	1	+	+ (3/4)
A11	66/M	PN/MC			–	– (0/4)
A12	61/M	PN/MC			–	– (0/4)
A13	84/F	sCJD	MM	1	+	+ (3/4)
A14	76/M	sCJD	MM	1	+	+ (2/4)
A15	69/M	sCJD	MV	1	+	+ (4/4)
A16	67/M	AD			–	– (0/4)
A17	75/F	PN/MC			+	– (0/4)
A18	93/M	DLB/PD			–	– (0/4)
A19	67/F	sCJD	ND	2	+	+ (2/4)
A20	53/M	DLB/PD			–	– (0/4)
A21	71/F	sCJD	VV	2	+	– (0/4)
A22	62/F	sCJD	MM	2	–	– (0/4)
A23	90/M	sCJD	VV	ND	+	+ (1/4)
A24	61/F	DLB/PD			–	– (0/4)
A25	74/M	sCJD	MM	ND	±[f]	+ (2/4)
A26	74/F	AD			–	– (0/4)
A27	68/F	sCJD	ND	ND	+	+ (2/4)
A28	69/F	sCJD	VV	2	+	+ (1/4)
A29	82/M	DLB/PD			+	– (0/4)
A30	70/F	sCJD	ND	2	+	+ (4/4)

[a]CJD can be divided into six molecular subtypes on the basis of whether methionine (M) or valine (V) is present at codon 129 of the gene encoding prion protein combined with the profile of PrP^{Sc} (type 1 or type 2) as determined by western blotting[17]. [b]Amounts of the γ-isoform of 14-3-3 protein in CSF were determined by western blotting with a polyclonal antibody specific for the γ-isoform of the 14-3-3 protein[18] (+, positive reaction; –, negative reaction). [c]RT-QUIC was performed as described in the **Supplementary Methods**. The number of positive reactions over the number of replicates is shown in parentheses. Samples with at least one positive reaction were defined as +, representing a positive result in the RT-QUIC. [d]The final diagnosis was made by the Australian National CJD Registry. [e]Amounts of 14-3-3 protein (all isoforms) in CSF were determined by western blotting. [f]Additional atypical bands were observed. [g]Kinetics graphs are provided in **Supplementary Figure 3.** Subjects or their families agreed with the aims and role of our research and gave appropriate informed consent. The investigation protocol was approved by the Ethics Committee of Nagasaki University Hospital (ID: 10042823), and the study was registered with the University Hospital Medical Information Network (ID: UMIN000003301). sCJD, sporadic Creutzfeldt-Jakob disease; iCJD, iatrogenic Creutzfeldt-Jakob disease; PN/MC, paraneoplastic/metastatic cancer; ICD, inflammatory central nervous system disorder; DLB/PD, dementia with Lewy bodies/Parkinson's disease; AD, Alzheimer's disease; ND, not determined.

These results indicate that RT-QUIC has the ability to discriminate CJD CSF samples that include 129MM, 129MV and 129VV cases from non-CJD CSF samples. In addition, none of the 130 Japanese cases of other neurological diseases were positive, further confirming the reliability of this assay (**Supplementary Table 4**). Collectively, the RT-QUIC assays showed more than 80% sensitivity and 100% specificity. The sensitivity was equivalent to and the specificity was much higher than that achieved by 14-3-3 (refs. 15,16), a nonspecific marker of rapid neuronal damage (**Supplementary Table 3**).

Although we have never experienced a false-positive reaction among the hundreds of non-CJD neurodegenerative disease samples we have so far tested, it remains possible that certain conditions may evoke a positive reaction, and further studies will be required to eliminate this possibility. Furthermore, scrupulous attention to the conditions of the assay is essential to avoid false positives in the clinical setting. Nevertheless, we believe that the ultrasensitive detection of PrP^{Sc} in CSF by RT-QUIC represents a valuable new means for the early, rapid and specific diagnosis of CJD.

Note: Supplementary information is available on the Nature Medicine website.

ACKNOWLEDGMENTS

We thank the members of the CJD Surveillance Committee in Japan for their support of this work, K. Yamaguchi and K. Kuwata for helping with the circular dichroism analysis of rPrP-sen, M. Tsujihata (Nagasaki Kita Hospital) for providing CSF samples and information about subjects and A. Yamakawa and A. Matsuo for technical assistance. The work was supported by the Global Centers of Excellence Program (F12); a grant-in-aid for science research (B; grant no. 20390287) from the Ministry of Education, Culture, Sports, Science and Technology of Japan; a grant for bovine spongiform encephalopathy research and a grant-in-aid of the Research Committee of Prion disease and Slow Virus Infection, from the Ministry of Health, Labor and Welfare of Japan.

AUTHOR CONTRIBUTIONS

R.A. designed the project, performed experiments and wrote the manuscript. K. Satoh, K. Sano, T.F., N.Y., D.I., T.M., T.N. and H.Y. performed experiments. K. Satoh, S.S., M.Y., H.M., T.K., G.K., A.M. and S.J.C. contributed to the collection of human specimens and provided information about subjects. N.N. supervised the project. K. Satoh, K. Sano, A.M., S.J.C. and N.N. helped with the editing of the manuscript.

COMPETING FINANCIAL INTERESTS

The authors declare no competing financial interests.

Published online at http://www.nature.com/naturemedicine/.
Reprints and permissions information is available online at http://npg.nature.com/reprintsandpermissions/.

1. Prusiner, S.B. *Proc. Natl. Acad. Sci. USA* **95**, 13363–13383 (1998).
2. Aguzzi, A. & Calella, A.M. *Physiol. Rev.* **89**, 1105–1152 (2009).
3. Lasmezas, C.I. *et al. Science* **275**, 402–405 (1997).
4. Gambetti, P. *et al. Ann. Neurol.* **63**, 697–708 (2008).
5. Saborio, G.P., Permanne, B. & Soto, C. *Nature* **411**, 810–813 (2001).
6. Castilla, J. *et al. Methods Enzymol.* **412**, 3–21 (2006).
7. Atarashi, R. *et al. Nat. Methods* **4**, 645–650 (2007).
8. Colby, D.W. *et al. Proc. Natl. Acad. Sci. USA* **104**, 20914–20919 (2007).
9. Atarashi, R. *et al. Nat. Methods* **5**, 211–212 (2008).
10. Orru, C.D. *et al. Protein Eng. Des. Sel.* **22**, 515–521 (2009).
11. Kocisko, D.A. *et al. Nature* **370**, 471–474 (1994).
12. Toth, S.I., Smith, L.A. & Ahmed, S.A. *J. Pharm. Sci.* **98**, 3302–3311 (2009).
13. Collins, S.R., Douglass, A., Vale, R.D. & Weissman, J.S. *PLoS Biol.* **2**, e321 (2004).
14. Lansbury, P.T. Jr. & Caughey, B. *Chem. Biol.* **2**, 1–5 (1995).
15. Hsich, G., Kenney, K., Gibbs, C.J., Lee, K.H. & Harrington, M.G. *N. Engl. J. Med.* **335**, 924–930 (1996).
16. Zerr, I. *et al. Ann. Neurol.* **43**, 32–40 (1998).
17. Parchi, P. *et al. Ann. Neurol.* **46**, 224–233 (1999).
18. Satoh, K. *et al. Lab. Invest.* **90**, 1637–1644 (2010).

FEBS Letters 584 (2010) 1193–1198

ELSEVIER

FEBS Letters

journal homepage: www.FEBSLetters.org

GABAA receptor subunit β1 is involved in the formation of protease-resistant prion protein in prion-infected neuroblastoma cells

Tomohiro Kimura [a], Kensuke Ishikawa [a,1], Yuji Sakasegawa [a], Kenta Teruya [a], Tetsutaro Sata [b], Hermann Schätzl [c], Katsumi Doh-ura [a,*]

[a] Department of Prion Research, Tohoku University Graduate School of Medicine, Sendai, Japan
[b] Department of Pathology, National Institute of Infectious Diseases, Toyama 1-23-1, Shinjuku, Tokyo 162-8640, Japan
[c] Institute of Virology, Prion Research Group, Technische Universität München, Trogerstr. 30, 81675 Munich, Germany

ARTICLE INFO

Article history:
Received 25 December 2009
Revised 5 February 2010
Accepted 11 February 2010
Available online 14 February 2010

Edited by Jesus Avila

Keywords:
Prion
GABAA receptor
gabrb1
siRNA
Antagonist

ABSTRACT

γ-Aminobutyric acid type A (GABAA) receptor β1 (gabrb1), a subunit of GABAA receptors involved in inhibitory effects on neurotransmission, was found to associate with the formation of protease-resistant prion protein in prion-infected neuroblastoma cells. Silencing of gabrb1 gene expression significantly decreased the abnormal prion protein level but paradoxically increased the normal prion protein level. Treatment with a gabrb1-specific inhibitor, salicylidene salicylhydrazide, dose-dependently decreased the abnormal prion protein level, but silencing of other GABAA receptor subunits' gene expression and treatments with the receptor antagonists and agonists did not. Therefore, gabrb1 involvement in abnormal prion protein formation is independent of GABAA receptors.

1. Introduction

Transmissible spongiform encephalopathies or prion diseases are fatal neurodegenerative disorders that include Creuzfeldt–Jakob disease in humans, and bovine spongiform encephalopathy and scrapie in animals. These diseases are characterized by deposition of a partially protease-resistant abnormal isoform of prion protein (PrPres), which is the main component of the pathogen and which is converted from the normal cellular isoform of prion protein (PrPc) in the central nervous system and lymphoreticular system [1]. Cell biology of the biosynthesis and metabolism of PrPc and PrPres has been eagerly investigated in prion-infected cells [2,3] but has not been fully elucidated. Especially, endogenous factors involved in the formation of PrPres or the conformational change from PrPc into PrPres [4,5] remain enigmatic.

Using gene screening by the gene silencing technique with small interfering RNA (siRNA) or short hairpin RNA (shRNA) [6,7], we have sought endogenous factors affecting the metabolism of PrPres in prion-infected neuroblastoma cells. We report here a possible linkage of γ-aminobutyric acid A receptor β1 (gabrb1) with the formation of PrPres. In fact, gabrb1 is a subunit of γ-aminobutyric acid type A (GABAA) receptors responsible for most of the fast inhibitory synaptic transmission in mammalian brain [8]. Belonging to the ligand-gated ion channels, they are formed by the pentameric assembly of homologous subunits. Numerous GABAA receptor subunits have been identified (α1–6, β1–3, γ1–3, δ, π, ε, and θ), all of which are products of separate genes, and most GABAA receptors contain two α subunits, two β subunits and either one γ subunit or one δ subunit [8]. It has been well documented that GABAergic neurons are affected by prion infection [9–15], but it is not clear whether GABAA receptors are involved in PrPres formation. Therefore, to address this query, we performed gene silencing experiments for gabrb1 and other representative GABAA receptor subunits (α5, β3, γ2, and δ) as well as GABAA receptor modulating experiments using the antagonists and agonists in prion-infected cells.

2. Materials and methods

2.1. siRNAs and compounds

Double-stranded siRNAs for GABAA receptor subunits used for this study (Table 1) were purchased from Invitrogen Corp. (Carlsbad, CA, USA). Some GABAA receptor antagonists (bicuculline

* Corresponding author. Address: Department of Prion Research, Tohoku University Graduate School of Medicine, 2-1 Seiryo-machi, Aoba-ku, Sendai 980-8575, Japan. Fax: +81 22 717 7656.
E-mail address: doh-ura@mail.tains.tohoku.ac.jp (K. Doh-ura).
[1] Present address: Department of Psychiatry, Saga University School of Medicine, Saga, Japan.

0014-5793/$36.00 © 2010 Federation of European Biochemical Societies. Published by Elsevier B.V. All rights reserved.
doi:10.1016/j.febslet.2010.02.029

methiodide and picrotoxin) and agonists (GABA, muscimol, and isoguvacine hydrochloride) were purchased from Sigma–Aldrich Corp. (St. Louis, MO, USA). Another agonist, pentobarbital, was purchased as a 5% (approximately 200 mM) solution of its sodium salt, nembutal, from Dainippon Sumitomo Pharma Co. Ltd. (Osaka, Japan). A specific inhibitor of GABAA receptor β1 subunit, salicylidene salicylhydrazide, was obtained from Tocris Bioscience (Missouri, USA).

2.2. shRNA expression vectors

The DNA fragments flanking 5′ *Bam*HI recognition sequence and 3′ *Hind*III recognition sequence, which corresponded to shRNA sequences for GABAA receptor subunits, were produced by annealing pairs of sense and antisense 64mer oligonucleotides, of which sense sequences were designed as follows: 5′-GATCC***GAgGGTGGAGTTCAtAAtAGG***CTTCCTGTCA***CCTGTTGTGAACTCCACCTTC***-TTTTTTA-3′ targeting to nucleotides 663–683 of β1 subunit coding sequence; 5′-GATCC***ACCTGGTgTGAtAGAtGTTTG***CTTCCTGTCA***CAAACGTCTGTCATACCAGGT***TTTTTTA-3′ targeting to nucleotides 355–375 of γ2 subunit coding sequence; 5′-GATCC***GAATGGGCTgCTTtACtATCC***CTTCCTGTCA***GGATGGTGAAGTAGCCCATTC***TTTTTTA-3′ targeting to nucleotides 809–829 of γ2 subunit coding sequence; 5′-GATCC***ACATGGAgTACACtATGAtTG***CTTCCTGTCA***CAGTCATGGTGATTTCCATGT***TTTTTTA-3′ targeting to nucleotides 245–265 of δ subunit coding sequence. Bold italic letters and small bold italic letters, respectively denote target sites and mismatch-induced sites. The DNA fragments were ligated into a pBAsi-hH1 (Takara Bio Inc., Shiga, Japan) cut with *Bam*HI and *Hind*III. The ligated vectors were introduced into *Escherichia coli*; then plasmids of interest were harvested and sequenced.

2.3. Mutated gabrb1 expression vector

Mouse gabrb1 gene was cloned from a ready mouse brain cDNA library (Marathon; Takara Bio Inc.) using PCR with KOD-plus DNA polymerase (Toyobo Co. Ltd., Osaka, Japan). A PCR product was inserted into a pcDNA3.1 Myc/His expression vector (Invitrogen Corp.). The ligated vectors were introduced into *E. coli*; then plasmids of interest were harvested and sequenced. Mutations were induced by site-directed mutagenesis using PCR technique with primers of 5′-GATGCATCTGCAGC*gc*G*t*GTgGC*t*CT*t*GG*t*AT*a*AC*a*AC-GGTGCTG-3′ (small italic letters indicate silent mutations induced) and 5′-TGCAGATGCATCATAGTTGATCCA-3′. The PCR products were treated with *Dpn*I for digesting template plasmids and introduced directly into *E. coli*; then plasmids of interest were harvested and sequenced.

2.4. Gene silencing experiments

Mouse neuroblastoma N2a cells infected persistently with RML prion strain (ScN2a) or 22L prion strain (N167) were diluted to 10% or 15% confluence with Opti MEM I (Invitrogen Corp.) including 10% fetal bovine serum (FBS), and 2.4 ml each was seeded onto six-well plates. Transfection was performed on the next day of seeding. TransFectin (3.0 μl/well; Bio-Rad Laboratories, Inc., Hercules, CA, USA) was used for the transfection of shRNA expression vectors, and siLentFect (3.0 μl/well, Bio-Rad Laboratories, Inc.) was used for transfection of double-stranded siRNAs. The amounts of vectors or siRNAs used in transfection were, respectively, 0.2 μg per well or 20 nM per well. Medium was changed on the day after transfection. Cells were harvested after washing with PBS 3 days after transfection.

Table 1
siRNAs and shRNAs used for this study.

GABAA receptor subunit examined	Nucleotide position of target region*	
	siRNA (catalog no.**)	shRNA
α5	311–335 (MSS201426)	
β1	820–844 (MSS204523)	663–683
β3	873–897 (MSS204527)	
β3 transcript variant 1	62–86 (MSS204528)	
γ2		355–375, 809–829
δ		245–265

* Nucleotide position in the coding sequence of each GABAA receptor subunit gene.
** siRNAs were obtained from Invitrogen Corp. (Carlsbad, CA, USA).

2.5. Rescue experiment

The ScN2a cells were diluted to 15% confluence with Opti MEM I including 10% FBS, and 2 ml each was seeded onto six-well plates. Transfection was performed on the day after seeding. TransFectin (2.0 μl/well) was used for the transfection of both mutated gabrb1 expression vector and double-stranded siRNA. The amounts of the vector and the siRNA used for transfection were, respectively, 0.8 μg per well and 5 nM per well. Medium was changed on the day after transfection. Cells were harvested after washing with PBS 3 days after transfection.

2.6. Immunoblotting

Cells were lysed with lysis buffer (0.5% sodium deoxycholate, 0.5% Nonidet P-40, PBS) after rinsed with PBS, and debris was eliminated by centrifugation at 3000×*g* for 10 min at 4 °C. Protein contents of each sample were measured using a modified Lowry method [16] with Dc protein assay reagent (Bio-Rad Laboratories, Inc.) with bovine serum albumin as a standard. For PrPres detection, cell lysate containing the same protein amount was treated with 10 μg/ml of proteinase K for 30 min at 37 °C, and PrPres was pelleted by centrifugation at 20 000×*g* for 20 min at 4 °C. After denaturation in sample buffer by heating at 95 °C for 10 min, PrP was separated using SDS–PAGE and then transferred onto Immobilon-P membrane (Millipore Corp., Bedford, MA, USA). Subsequently, PrP was detected using a monoclonal antibody SAF83 as a primary antibody, which recognizes residues 126–164 of mouse PrP (1:5000; SPI-Bio, Massy, France), and an alkaline phosphatase-conjugated goat anti-mouse antibody (1:20 000; Promega Corp., Madison, WI, USA) as a secondary antibody. Immunoreactivity was visualized using CDP-Star detection reagent (Amersham, Piscataway, NJ, USA) and was analyzed densitometrically using the ImageJ program (National Institutes of Health, Bethesda, MD, USA). To check the sample integrity, protein levels of GAPDH and β-actin were analyzed in the same samples used for PrPres detection.

2.7. Quantification of mRNA level

Cells were lysed with RNAiso-plus reagent (Takara Bio Inc.). Total RNA was extracted using FastPure RNA (Takara Bio Inc.). Poly A^+ RNA was purified from total RNA using an isolation kit (MicroFast Track MAG micro mRNA; Invitrogen Corp.). In addition, cDNA was synthesized with first strand cDNA synthesis kit (Takara Bio Inc.). The mRNA level was measured by real-time PCR using SYBR Premix Ex Taq II (Takara Bio Inc.) or using TaqMan probe with gene expression assay master mix for gabrb1 (Mm00433461_m1; Applied Biosystems). Fold change of gene expression was calculated using the $2^{-\Delta\Delta Ct}$ method, with GAPDH as an internal control.

2.8. Statistical analyses

Statistical significance was analyzed using one-way analysis of variance followed by the Tukey–Kramer post-hoc test for multiple

sample comparisons, or using a *t*-test for the two sample comparisons. Statistical significance for each analysis was defined as $P < 0.05$.

3. Results

3.1. Effects of gabrb1 gene silencing

Gene silencing of gabrb1 in ScN2a cells by transfection of shRNA expression vector targeting at nucleotides 663–683 of gabrb1 coding sequence demonstrated a significant decrease in both gabrb1 mRNA level (Fig. 1a) and PrPres formation (Fig. 1b). On the other hand, the PrP mRNA level increased significantly (Fig. 1a); upregulation in PrPc protein level was confirmed in uninfected N2a cells as well as ScN2a cells (Fig. 1a and c). Similar results were also observed in the gene silencing experiment using double-stranded siRNA, which was designed to target at nucleotides 820–844 of gabrb1 coding sequence (Fig. 1d–f). Protein levels of GAPDH and β-actin in the cells treated with the gabrb1 shRNA or siRNA were consistent with those of the mock controls (Fig. 1b and e), indicating that the reduction of PrPres level was not attributable to either sample preparation artifacts or cell viability difference. On the other hand, in comparison with ScN2a cells, N167 cells showed a less remarkable decrease in PrPres formation when treated with the gabrb1 siRNA (Supplementary Fig. 1).

Other representative subunits of GABAA receptor, including β3 and one of its transcript variants, as well as α5, γ2, and δ, were subjected to gene silencing experiments in ScN2a cells, but no modification in the PrPres level was observed despite marked reduction in mRNA levels of the target genes (Supplementary Fig. 2). These subunits were chosen from the following facts. Most GABAA receptors contain two α subunits, two β subunits, and either one γ subunit or one δ subunit [8]. The α5 subunit is reportedly upregulated in the brain when prion is inoculated into the mice expressing anchorless PrP [17]. The β3 subunit is the most abundant β subunit observed in ScN2a (data not shown). The γ2 subunit is the most abundant subunit in the brain and is incorporated in most GABAA receptor subtypes [18]. The δ subunit comprises only one member. In addition to the subunits described, the β2 subunit was also examined in this study, but its gene silenc-

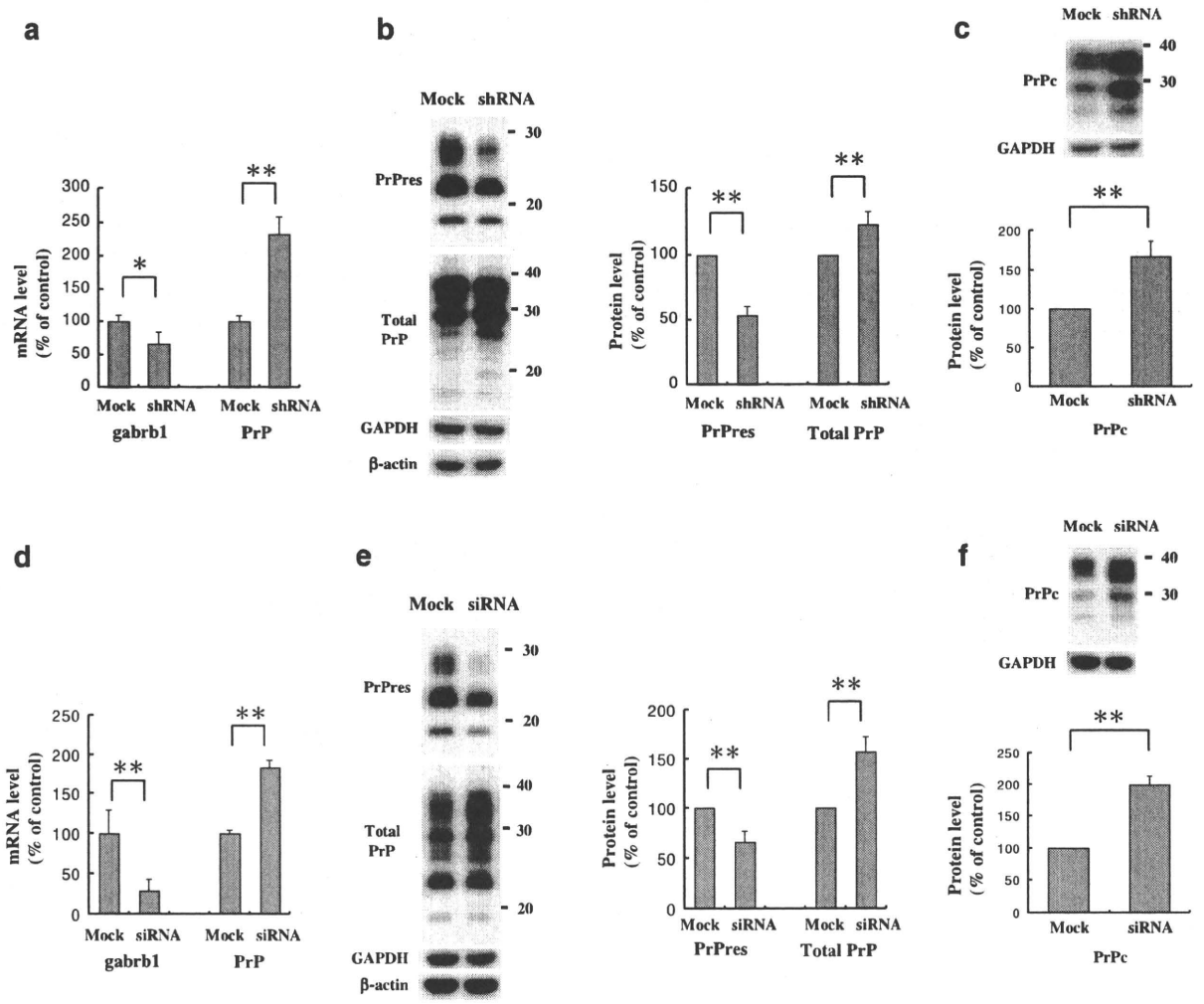

Fig. 1. Effects of gabrb1 gene silencing. Data from ScN2a cells transfected with shRNA expression vector or mock vector are shown: mRNA level of gabrb1 and PrP (a); immunoblot and protein level of PrPres and total PrP (b). Immunoblot and protein level of PrPc from N2a cells transfected with shRNA expression vector or mock vector are shown in (c). Data from ScN2a cells transfected with double-stranded siRNA or transfection reagent only (mock) are shown: immunoblot and protein level of PrPres and total PrP (d); mRNA level of gabrb1 and PrP (e). Immunoblot and protein level of PrPc from N2a cells transfected with double-stranded siRNA or transfection reagent only (mock) are shown in (f). Molecular size markers in the right side of the immunoblots are shown in kilodaltons. Immunoblot data shown here are representative examples; the graphic data shown here are the average and standard deviation from results of independent triplicate experiments ($^{*}P < 0.05$, $^{**}P < 0.01$).

ing effects were not evaluated because of its very low gene expression level in ScN2a cells.

3.2. Rescue of gene silencing effect

To confirm the specificity of gabrb1 gene silencing, a rescue experiment was performed using an expression vector for the mutated gabrb1 gene, which contained silent mutations at the targeting region of the double-stranded siRNA. Introduction of this mutated gabrb1 gene into ScN2a cells did not modify the PrPres level (Fig. 2; lanes 1 and 2). Co-transfection of the mutated gabrb1 expression vector and the double-stranded siRNA into ScN2a cells caused no reduction of the PrPres level, although co-transfection of the mock expression vector and the double-stranded siRNA caused substantial reduction in the PrPres level (Fig. 2; lanes 3 and 4). Consequently, the gabrb1 gene silencing effect on the PrPres formation was rescued by the expression of the silent mutation-containing gabrb1 gene.

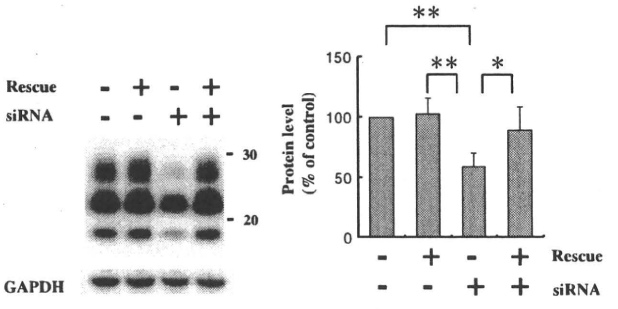

Fig. 2. Rescue of gabrb1 gene silencing. Immunoblot and protein level of PrPres from ScN2a cells transfected with silent mutation-containing gabrb1 expression vector (rescue +) or mock vector (rescue −) in the presence of (siRNA +) or the absence of (siRNA −) the siRNA used in the experiment shown in Fig. 1. Molecular size markers in the right side of the immunoblots are shown in kilodaltons. Immunoblot data shown here are representative examples; the graphic data shown here are the average and standard deviation from results of independent triplicate experiments (*$P < 0.05$, **$P < 0.01$).

3.3. Effects of GABAA receptor-related compounds

Salicylidene salicylhydrazide is a selective inhibitor of β1 subunit-containing GABAA receptors [19]. Treatment of ScN2a cells with this compound inhibited PrPres formation dose-dependently with a 50% inhibition dose of 450 nM (Fig. 3a). However, it did not modify the PrP mRNA level and the PrPc level, as demonstrated in the experiment using N2a cells (Supplementary Fig. 3). Another GABAA receptor antagonist, bicuculline methiodide [8], was also effective in inhibiting the PrPres formation dose-dependently but at almost a thousand times higher dose than that of salicylidene salicylhydrazide (Fig. 3b). No other GABAA receptor-related compound modified the PrPres level in ScN2a cells (Supplementary Fig. 4). The compounds tested in this study included an antagonist, picrotoxin [8], and agonists such as GABA [8], muscimol [8], pentobarbital [8], ethanol [20], and isoguvacine hydrochloride [21].

4. Discussion

Results show that gabrb1 is involved in the PrPres formation in ScN2a cells. The PrPres level was reduced significantly by gabrb1 gene silencing using either shRNA or siRNA, designed to target each different region of the gene. This gabrb1 gene silencing effect was rescued by co-transfection of silent mutation-containing gabrb1 gene, which was designed not to be targeted by the siRNA. Moreover, the results of the experiment with gabrb1-specific inhibitor salicylidene salicylhydrazide were coincident with those of gabrb1 gene silencing experiments. These results indicate that gabrb1 gene silencing effects are not artifacts such as off-targeting. We confirmed the gabrb1 gene silencing effects in the mRNA level but not in the protein level. We attempted unsuccessfully to detect gabrb1 in protein level using several gabrb1-specific antibodies ob-

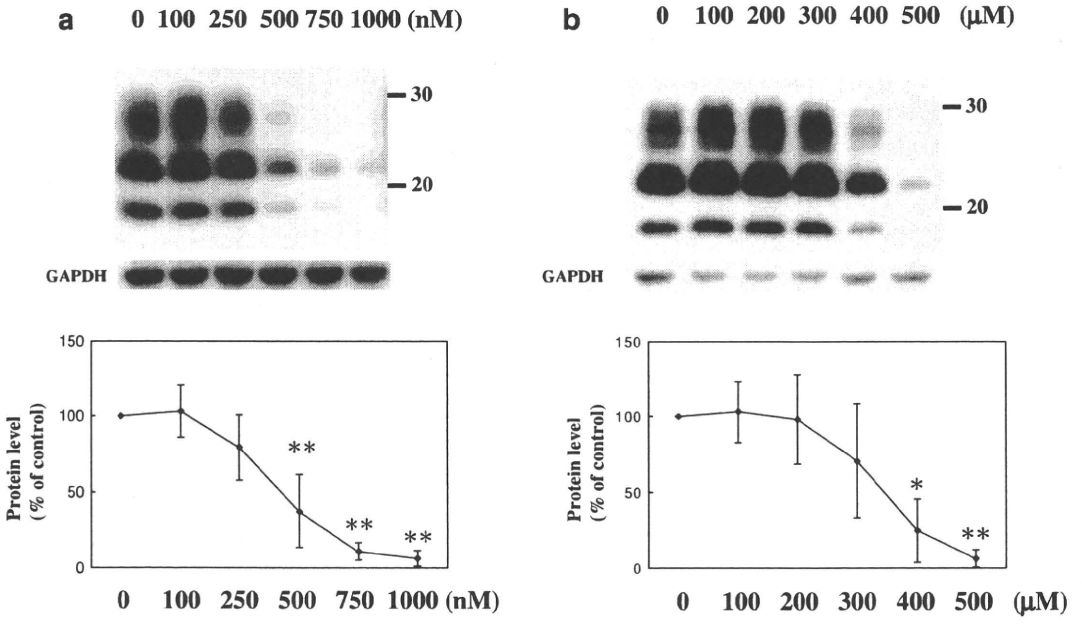

Fig. 3. Effects of gabrb1-specific inhibitor and GABAA receptor antagonist. Immunoblot and protein level of PrPres from ScN2a cells treated with gabrb1-specific inhibitor salicylidene salicylhydrazide (a) or GABAA receptor antagonist bicuculline methiodide (b) are shown. Molecular size markers in the right side of the immunoblots are shown in kilodaltons. Immunoblot data shown here are representative examples; the graphic data shown here are the average and standard deviation from results of independent triplicate experiments (*$P < 0.05$, **$P < 0.01$).